1963

The effect of combined moment and shear on the formation of plastic hinges in reinforced concrete beams

Edward James Rhomberg
Iowa State University

THE EFFECT OF COMBINED MOMENT AND SHEAR ON THE FORMATION OF PLASTIC HINGES IN REINFORCED CONCRETE BEAMS

by

Edward James Rhomberg

A Dissertation Submitted to the
Graduate Faculty in Partial Fulfillment of
The Requirements for the Degree of
DOCTOR OF PHILOSOPHY

Major Subject: Structural Engineering

Approved:

Signature was redacted for privacy.

In Charge of Major Work

Signature was redacted for privacy.

Head of Major Department

Signature was redacted for privacy.

Dean of Graduate College

Iowa State University
Of Science and Technology
Ames, Iowa

1963

TABLE OF CONTENTS

INTRODUCTION

Object

In the analysis of statically indeterminate structures by the principles of limit-load theory, plastic hinges are assumed to form at points of maximum moment, the members between hinges remaining elastic. These plastic hinges are zones of yielding which form as the load on the statically indeterminate structure is increased toward the ultimate. If deformations are limited by portions of the structure which are still elastic, a redistribution of moments will take place with the less-highly stressed portions of the structure carrying increased moments.

The successful redistribution of moments requires that a certain amount of angular rotation be available at a zone of yielding. For structures of reinforced concrete this rotation capacity is a matter of great importance since the ultimate strain for concrete may be small.

Many of the past investigations of the rotation capacity and ultimate moment of reinforced concrete beams have taken little or no account of the shear present at the section. Present engineering practice in the United States, as evinced in the Building Code of the American Concrete Institute (1), recognizes only the bending moment and axial

load existing at a cross section as contributing to the formation of zones of yielding. There is, however, experimental evidence which indicates that the effect of shear is not always negligible. Brock (2) stated that the effects of shear may cause collapse at loads much smaller than those necessary for the development of plastic hinge mechanisms. He also pointed out that, where shear is important, the plastic theory may be expected to overestimate seriously the strength of concrete members.

The primary objective of this research was to determine the influence of combined bending moment and shear on the plastic rotation available in reinforced concrete members. A secondary objective of the investigation was the development of a method of computing deflections and rotations of reinforced concrete beams, which method would include the effect of shear.

The scope of the investigation was limited to beams which failed in flexure.

Outline of Tests

Twenty-seven singly-reinforced concrete beams were tested. A beam-column connection was used in order to approximate the condition occurring in continuous frames where plastic hinges form. The parameters were the percent-

age of longitudinal reinforcement, the amount of web reinforcement, and the shear span. Concrete strength was not intentionally made a variable.

Load was applied continuously to the beams without stopping to make observations. Measurements of strains in the longitudinal reinforcement and on the concrete surface were made on continuous strain recorders. The beams were photographed at intervals with specially made cameras. Deflections as observed on dial gages were read from the negatives and rotations were measured from the negatives.

The beams are identified by two numbers and one letter, such as 8-1-A. The first number denotes the nominal shear span to depth ratio and the second number the approximate percentage of longitudinal reinforcement. The letter establishes the amount of web reinforcement.

The tests were conducted in the Engineering Experiment Station Laboratory of Iowa State University.

Notation

The following notation is used:

x, y, z	Coordinate axes
f	Normal unit stress in concrete
f'_c	Compressive strength of 6- by 12-inch concrete cylinders

f_s	Unit stress in tension reinforcement
v	Shearing unit stress in concrete
v'_c	Shearing strength of concrete
ϵ	Normal unit strain in concrete
ϵ_o	Normal unit strain in concrete at maximum normal stress; see Figure 4
ϵ_c	Normal unit strain at outer fiber of cross section
ϵ_s	Unit strain in tension reinforcement
ϵ_{so}	Unit strain in tension reinforcement at start of strain hardening
γ	Shearing unit strain in concrete
γ_o	Shearing unit strain at maximum shearing stress
γ_{kd}	Shearing unit strain at neutral axis
b	Width of cross section
d	Distance from centroid of tension reinforcement to compression face of beam
A_s	Area of tension reinforcement
L	Length from face of column to support
s	Distance measured downward from compression face of beam
y	Distance measured from neutral axis
$\bar{y}$	Distance to centroid of normal compressive stress measured from neutral axis
kd	Depth of compression zone of concrete
C	Internal compressive force in concrete
T	Tensile force in reinforcement
V	Shearing force in concrete

M	Bending moment
u	Strain energy per unit volume
U_s	Strain energy at yield due to stress in tensile reinforcement
u_c	Strain energy at yield per unit volume due to normal stress in concrete
U_c	Strain energy at yield due to normal stress in concrete
u_v	Strain energy at yield per unit volume due to shearing stress in concrete
U_v	Strain energy at yield due to shearing stress in concrete
U_T	Total strain energy at yield
W_s	Strain energy at ultimate in tensile reinforcement
W_c	Strain energy at ultimate in concrete due to normal stress
W_v	Strain energy at ultimate in concrete due to shearing stress
W_T	Total strain energy at ultimate
E_s	Modulus of elasticity of tensile reinforcement
E_c	Initial tangent modulus of elasticity of concrete
G_c	Modulus of rigidity of concrete
e	Natural logarithm base
m	Distance limiting spread of plasticity, measured from face of column
p	Ratio of $\frac{A_s}{bd}$
Δ_y	Deflection at yield load
Δ_u	Deflection at ultimate load
θ_p	Concentrated plastic rotation

The letters y and u, when subscribed to the above symbols, refer to the yield and ultimate conditions, respectively.

Review of Earlier Research

The work of A. L. L. Baker at the Imperial College in London has been directed toward limit design of reinforced concrete members. He developed (3) a method of computing the amount of moment redistribution in continuous beams in which the slope of a beam loaded to the plastic range could be expressed as $\int \frac{M\,ds}{EI}$, if appropriate values of EI at the elastic and plastic stages were used. Baker also recommended limiting values of the plastic strain of concrete and the length of material subject to yield. His recommendations were based on tests of statically determinate members.

Chan (4) discussed the relationship between the plastic hinge rotations and the developed plasticity in plastic hinge sections. The length of material subject to yield was shown to be a function of the shape of the bending moment diagram and the moment-strain curve of the section. Chan concluded that lateral restraint, such as spirals placed at the hinge section, could increase the amount of rotation available.

Ernst (5) conducted an investigation to determine the amount of concentrated plastic rotation developed at thirty-three simulated beam-column connections. His beams were 6 by 12 inches in cross section, with a span of 9 feet. Column stubs 9 1/2 inches high and 6 inches wide and of varying length were cast integrally on top and bottom of each beam at midspan. Load was applied to the beams through the column stubs. Other variables were the percentage of longitudinal tension reinforcement and the rate of loading. The beams were tested in a 400,000 pound hydraulic testing machine with fixed loading head. Strains on the tension reinforcement and on the top concrete surface were measured with SR-4 electric strain gages. Deflections were measured by means of an engineer's level sighted on scales attached at midspan. Ernst concluded that the amount of plastic rotation increases with decreasing percentage of steel.

MATERIALS AND TEST SPECIMENS

Materials

Type III Portland cement was used in all beams. The cement was purchased in two lots from the manufacturer, Hawkeye-Marquette Cement Co., West Des Moines, Iowa, and was stored in paper bags for about five days until used.

The fine and coarse aggregates used in all beams were obtained from a glacial deposit adjacent to the Raccoon River at West Des Moines, Ia. The fineness modulus of the fine aggregate was 3.05. The coarse aggregate had a maximum size of 3/8 inch and a fineness modulus of 5.98. The fine aggregate met the grading requirements of specification C33-61T of the American Society for Testing Materials. Sieve analyses are given in Table 1.

Table 1. Sieve analyses of aggregate

	Percentage retained on sieve size							
	$\frac{1}{2}$ inch	$\frac{3}{8}$ inch	#4	#10	#16	#30	#50	#100
Fine	0	0	1.8	20.8	42.1	59.4	83.3	97.4
Coarse	0	7.3	97.9	99.6	99.8	100	100	100

The longitudinal reinforcement was structural grade

deformed bars of three sizes: #3, #4, and #5. All bars were purchased from the same commercial firm but were not of the same heat. Stress-strain curves as determined from tension tests are given in Figure 1.

The web reinforcement, obtained in one lot from the supplier, was a soft, black annealed wire. The sizes used ranged from 6AWG to 15AWG. The wire was tested in the laboratory and the properties are given in Table 2.

Table 2. Properties of web reinforcing

Size AWG[a]	Diameter inch	Yield point ksi
6	0.177	25.0
9	0.148	30.0
10	0.135	32.5
11	0.120	28.5
12	0.105	34.5
13	0.091	31.0
14	0.080	25.0
15	0.072	32.0

[a]American Wire Gage.

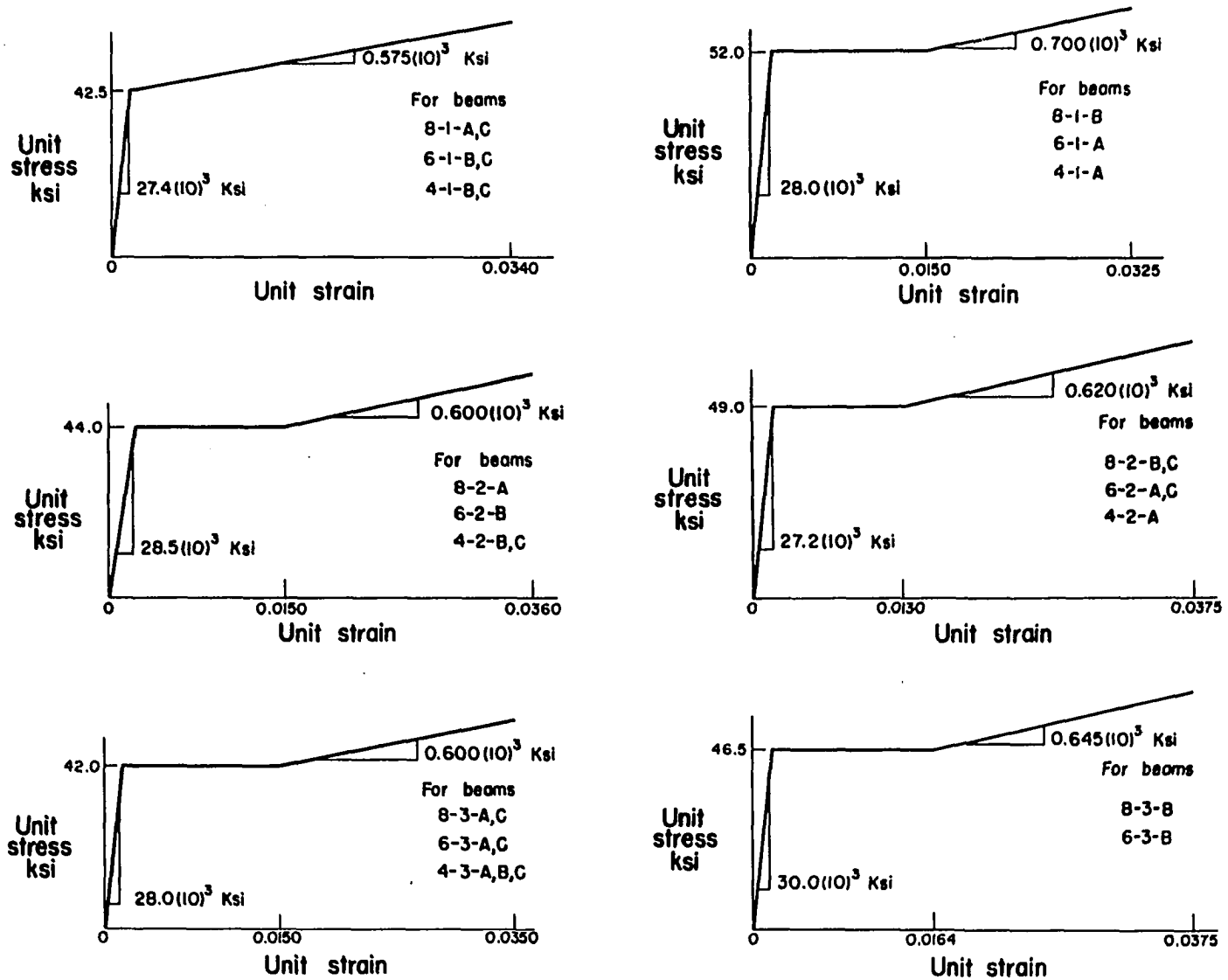

Figure 1. Stress-strain curves for longitudinal reinforcement

Description of Specimens

All beams were rectangular in cross section and were singly reinforced. The beams were nominally 3 inches in width and 7 inches in total depth. The span lengths were chosen to give ratios of shear span to depth of 8, 6, and 4. A beam-column connection configuration was employed to simulate the conditions under which plastic hinges form in concrete frames.

Closed-loop stirrups were provided at a spacing of 3 inches in all beams. The stirrups were designed to carry approximately 100 per cent, 67 per cent and 50 per cent of the shear at working loads. In a beam series such as 8-1-A, 8-1-B, and 8-1-C, the letter A denotes the larger amount of web reinforcing and the letter C the smaller amount.

Dimensions and other data pertaining to the beams are given in Tables 3 and 4. A beam as set up in the testing machine is shown in Figures 2 and 3.

Casting and Curing of Specimens

All beams were cast on their sides in oil-treated wood forms. Longitudinal reinforcing steel was held from the side of the form by 1/2-inch lengths of 1/2-inch diameter steel rod. Stirrups were securely wired to the longitudinal

Table 3. Concrete strengths

Cast	Beam	Number of cylinders tested	f'_c		Where cast
1	8-1-A,C 8-2-A 8-3-A,C 6-2-B 6-3-A,C	11	6200		West Des Moines
2	6-1-B,C 4-1-B,C 4-2-B,C 4-3-A,B,C 2-1-A,B,C 2-2-A,B,C 2-3-A,B,C	27	6400		West Des Moines
3	8-1-B	3	5180	f'_c avg = 5200	Ames
	8-2-B	3	5000		
	8-2-C	3	5430		
	8-3-B	3	5220		
	6-1-A	3	5240		
	6-2-A	3	5290		
	6-2-C	3	5040		
	6-3-B	3	5330		
	4-1-A	3	5110		
	4-2-A	3	5170		
4	6-2-B	3	4400		Ames

steel and to nails which were driven into the bottom of the forms so as to hold up the stirrups.

The beams were cast at three different times. Casts one and two were made with the facilities of Midwest Concrete

Table 4. Properties of beams

Beam	L inch	b inch	d inch	f'_c psi	A_s sq.in.	Web steel AWG
8-1-A	50.5	3.05	6.31	6200	2-#3	11
8-1-B	50.5	3.00	6.31	5200	2-#3	13
8-1-C	50.5	3.03	6.34	6200	2-#3	15
8-2-A	50.0	3.00	6.25	6200	2-#4	11
8-2-B	50.0	3.00	6.25	5200	2-#4	13
8-2-C	50.0	3.00	6.25	5200	2-#4	15
8-3-A	49.5	3.00	6.19	6200	2-#5	10
8-3-B	49.5	3.00	6.22	5200	2-#5	12
8-3-C	49.5	3.00	6.19	6200	2-#5	14
6-1-A	37.9	3.00	6.31	5200	2-#3	11
6-1-B	37.9	3.00	6.31	6400	2-#3	13
6-1-C	37.9	3.00	6.31	6400	2-#3	15
6-2-A	37.5	3.00	6.25	5200	2-#4	9
6-2-B	37.5	3.00	6.22	4400	2-#4	11
6-2-C	37.5	3.00	6.25	5200	2-#4	13
6-3-A	37.1	3.09	6.19	6200	2-#5	9
6-3-B	37.1	3.00	6.19	5200	2-#5	11
6-3-C	37.1	3.03	6.19	6200	2-#5	13
4-1-A	25.2	2.97	6.31	5200	2-#3	10
4-1-B	25.2	3.03	6.31	6400	2-#3	12
4-1-C	25.2	3.00	6.31	6400	2-#3	14
4-2-A	25.0	3.00	6.25	5200	2-#4	6
4-2-B	25.0	3.00	6.25	6400	2-#4	9
4-2-C	25.0	3.03	6.31	6400	2-#4	11
4-3-A	24.8	2.94	6.19	6400	2-#5	6
4-3-B	24.8	3.05	6.25	6400	2-#5	9
4-3-C	24.8	3.00	6.19	6400	2-#5	11

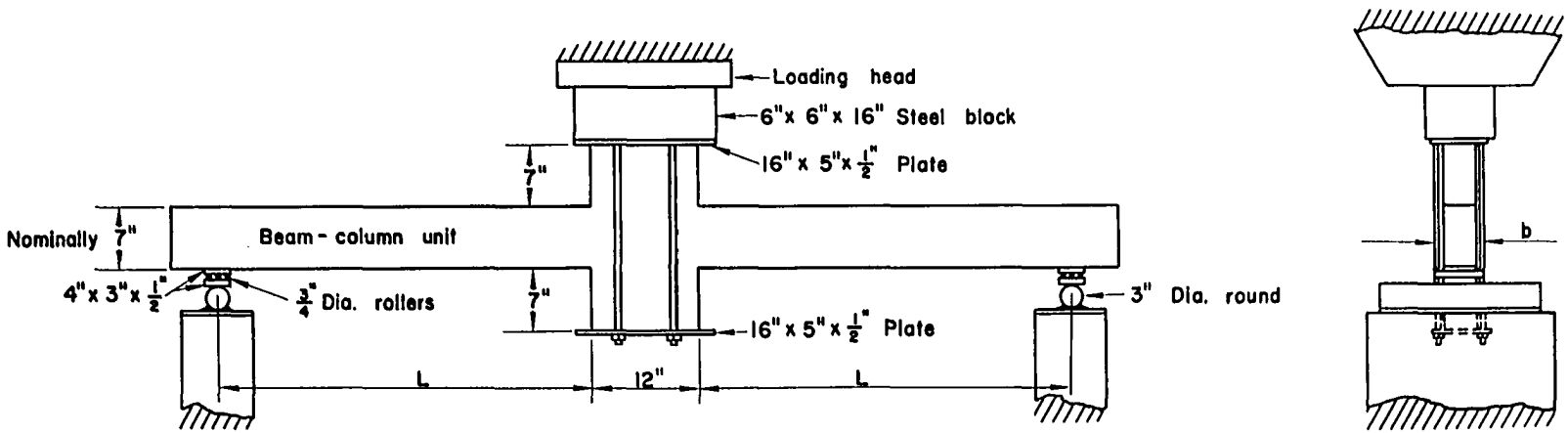

Figure 2. Beam test setup

Figure 3. Photograph of beam test setup

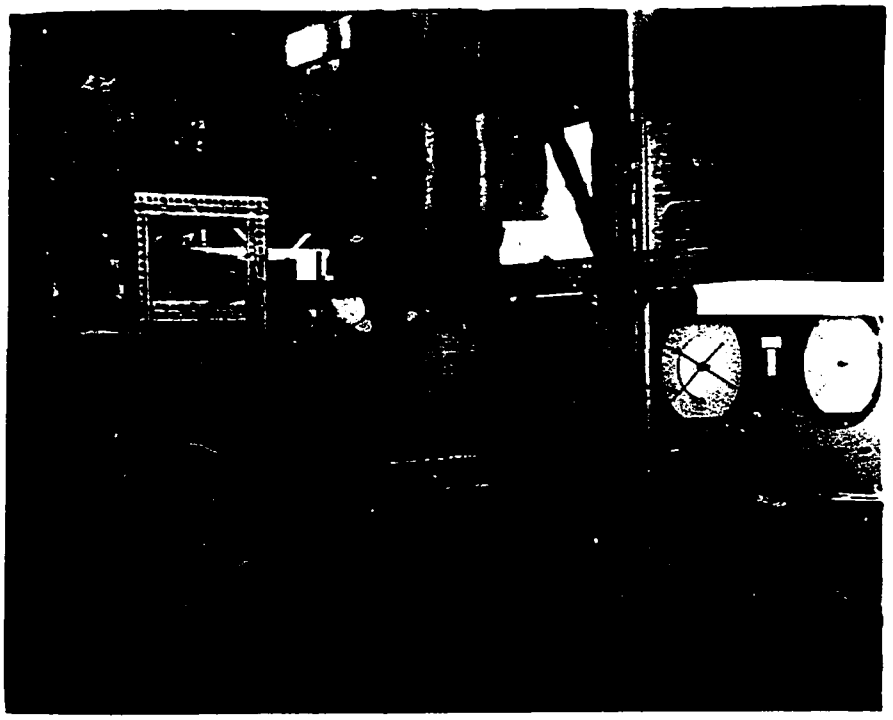

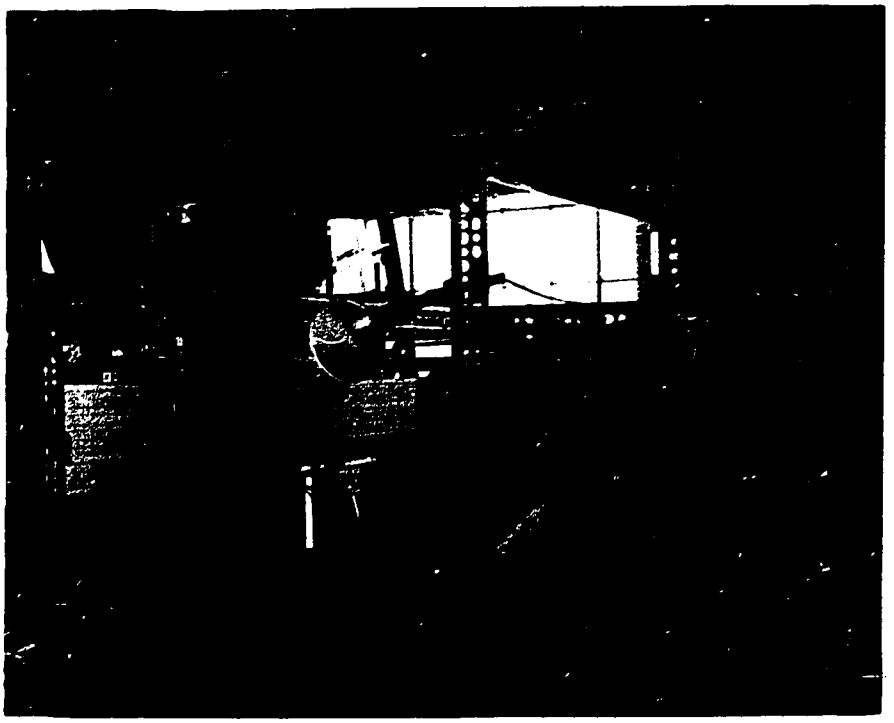

Industries in West Des Moines, Iowa. There, the concrete was mixed in a non-tilting, bottom-dump, drum mixer of 1 cubic yard capacity. The concrete was shoveled into the forms and the forms were shaken on a vibration table.

The third casting was made in the laboratory. The concrete was mixed in a tilting, rotating drum mixer of 3 cubic foot capacity. A high-frequency internal vibrator was used to aid in placing the concrete in the beams.

The same basic concrete mix was used for all beams, except 6-2-B, in an effort to obtain the same concrete strength. That this was not achieved is attributed to differences in cement quality and moisture content of the aggregate. Beam 6-2-B was originally cast as a trial beam but was pressed into service when its counterpart proved to be defective. The strengths of the batches are given in Table 3.

Several hours after casting, the beam surfaces were troweled smooth. The beams, and the 6- by 12-inch control cylinders which were cast with the beams, were covered with strips of burlap which were moistened periodically during the next seven days. The beams and cylinders were removed from the forms seven days after they were cast and were then stored in the air in the laboratory until tested. The age of the beams at testing varied from five to seven months.

INSTRUMENTATION, LOADING APPARATUS, AND TEST PROCEDURE

Electric Strain Gages and Recorders

Strain measurements were made on the reinforcing steel to define clearly the stage of first yielding. Measurements were also made at the top surfaces of the beams to determine the longitudinal distribution of strain in the concrete at failure. The strains were measured by SR-4 electrical resistance gages, types A-1 and A-12. Five A-1 gages, which have a nominal gage length of 13/16 inch, were placed on the top surface of each beam from 5/8 inch to 8-1/2 inches from the column face. Three gages were used on one side of the column and two on the other in some instances; in others, all five gages were used on one side. One A-12 strain gage, with a nominal gage length of 1 inch, was attached to each of the two reinforcing bars through core holes blocked out before the beams were cast. One gage was used on each side of the column. The steel reinforcing bars were prepared before casting of concrete by filing off the deformations for about a 2 inch length and by covering the smooth surface with a piece of electrical tape and a block of sponge rubber. All SR-4 gages were attached with Duco cement without application of heat. Several days elapsed between attachment of gages and testing of the beams.

A continuous record of strain was produced by Brush universal amplifiers (BL-520) and Brush direct-writing recorders (BL-274). The Brush universal amplifiers have attenuator settings which vary from 1 microinch per inch of strain per attenuator-line to 1000 microinch per inch of strain per attenuator-line, allowing wide selection of amplification of strain.

Deflection Measurements

Measurements of the vertical displacement of each side of the column stub relative to the supports of the beams were obtained from dial gages. The gages were supported by a deflection bridge and were actuated by short lengths of angle cemented to the column stub. Readings of the dials were recorded on photographic film. To obviate halting the test and resetting the dials, two dials were used on each side of the column and were staggered so that one was always in operation when the movement of the other was expended.

Photographic Equipment

Two specially designed cameras were used to photograph the beams in areas where large cracks were expected to open. The cameras employ metrogon lens systems which are wide-angle

lenses possessing very small distortion. The lenses were fitted to Fairchild F-56 roll film magazines using a 7 inch wide roll of film. Kodak Plus X, Aerecon, Type 1B film was used in the tests. According to the manufacturer, the film has a shrinkage of approximately one part in 25,000. In order to more easily define the edges of a crack on the negative, the surfaces of the beams were very lightly coated with a mixture of plaster of paris and water. The cameras were positioned so that approximately a 21 inch length of a beam could be photographed and also so that the dial gages measuring deflection would be included in the photograph. This resulted in a scale of approximately 3 to 1 (i.e., 3 inches on the beam equal about 1 inch on the negative). Comparison of crack widths measured on the beam with those measured on the negative showed accuracies of plus or minus 0.001 inch (6).

Loading Apparatus

All beams were tested in a 400,000-pound capacity Southwark-Emery hydraulic testing machine equipped with loading beams. Since the load was applied off-center of the testing machine, Figure 3, the load-measuring device was compared against a previously calibrated load cell for the range of loads to be used and was found to be satisfactory.

The load was applied to the top of the column stub through a steel block 6 by 6 by 16 inches which was bolted in a fixed position to the loading head.

The steel block acted against the upper steel plate of a clamping device, Figure 2, designed to simulate the condition of a loaded column for the column stub of the specimens. The equivalent of a uniform vertical pressure of approximately 300 pounds per square inch was applied to the column stub by drawing the nuts on the bolts tight to a specified value with a torque wrench. The reactions at both supports were developed by hard steel plates and rollers, Figure 2, thus permitting horizontal movement and rotation. A thin layer of plaster of paris between all steel plates and concrete bearing areas was used to develop a more uniform bearing pressure.

Test Procedure

The tests were begun after the amplifiers, cameras, and dial gages were readied. Load was applied continuously to failure, with photographs by both cameras being taken at increments of load up to initial yielding of steel and at increments of steel strain thereafter. These instantaneous measurements eliminated drop-off of load and change of deflection while measurements were made. The timing of

measurements was coordinated by vocal signal. Load was applied to the beams until they ruptured completely or failed to develop increased resistance to increased deformation. The length of time required to test the beams varied from 30 minutes for the longer span beams to 10 minutes for the shorter span beams.

ANALYTICAL STUDIES

Conditions at Yield Load

The bending moment in a singly reinforced concrete beam, when the steel reaches the yield point, may be evaluated if the location and magnitude of the internal forces are known. The magnitude of the compressive and tensile forces is equal to the yield stress of the reinforcing steel multiplied by the area of the steel. The location of the resultant compressive force on the concrete may be determined if the distribution of the compressive stress is known.

The relation between stress and strain as determined from concentric compression tests of concrete cylinders has been applied to the flexural compression occurring in beams by assuming a linear distribution of strains in the compression region. Smith and Young (3) have shown that a single continuous function

$$f = f'_c \frac{\epsilon}{\epsilon_o} e^{1 - \frac{\epsilon}{\epsilon_o}} \qquad (1)$$

may be used to compute the compressive force, the position of neutral axis, and the moment. The function covers the full range of stress, including the descending portion beyond

maximum stress, and depends upon the properties of the concrete as determined from cylinder tests.

In applying the exponential function to the beams of this investigation, the assumptions were made that the concrete carried no tensile stress and that the maximum stress occurred at a unit strain of 0.002. This last assumption is supported by the cylinder tests of this investigation as well as those of Smith and Young (7) and Ramaley and McHenry (8).

The cylinder tests of this study were carried as far as the ultimate load only. Whitney (9) and Hognestad, Hanson, and McHenry (10) indicate that the abrupt failure of cylinders is related to properties of the testing machine rather than to properties of the concrete. Smith and Young (7) show that the exponential function approximates closely that portion up to a unit strain of 0.004 of the concrete cylinder stress-strain curves as presented by Ramaley and McHenry (8). It was assumed for the purposes of this investigation that the curing conditions of the concrete in the beams and the strain rate applied were such that the stress distribution in the concrete of the beams could be represented by the exponential function.

The exponential function is plotted in Figure 4 with a typical stress-strain curve from a cylinder test of this investigation shown for comparison purposes.

When the reinforcing steel reaches the yield point,

the neutral axis, on consideration of Figure 5, may be located as follows:

$$C_y = b\int_0^{k_y d} f\, dy = f_{sy}\, A_s$$

where $\frac{\epsilon}{y} = \frac{\epsilon_{sy} + \epsilon_{cy}}{d}$ and $dy = \frac{d}{\epsilon_{sy} + \epsilon_{cy}}\, d\epsilon$

Then $f_{sy}\, A_s = \frac{bd}{\epsilon_{sy} + \epsilon_{cy}} \int_0^{\epsilon_{cy}} f\, d\epsilon$

Substituting f from Equation 1, integrating between limits, and simplifying give

$$C_y = f_{sy}\, A_s$$

$$= \frac{bd\, f'_c}{\epsilon_{sy} + \epsilon_{cy}} \left[(\epsilon_o + \epsilon_{cy}) \left(- e^{1 - \frac{\epsilon_{cy}}{\epsilon_o}}\right) + \epsilon_o e \right] \qquad (2)$$

Since ϵ_o has been assumed equal to 0.002, Equation 2

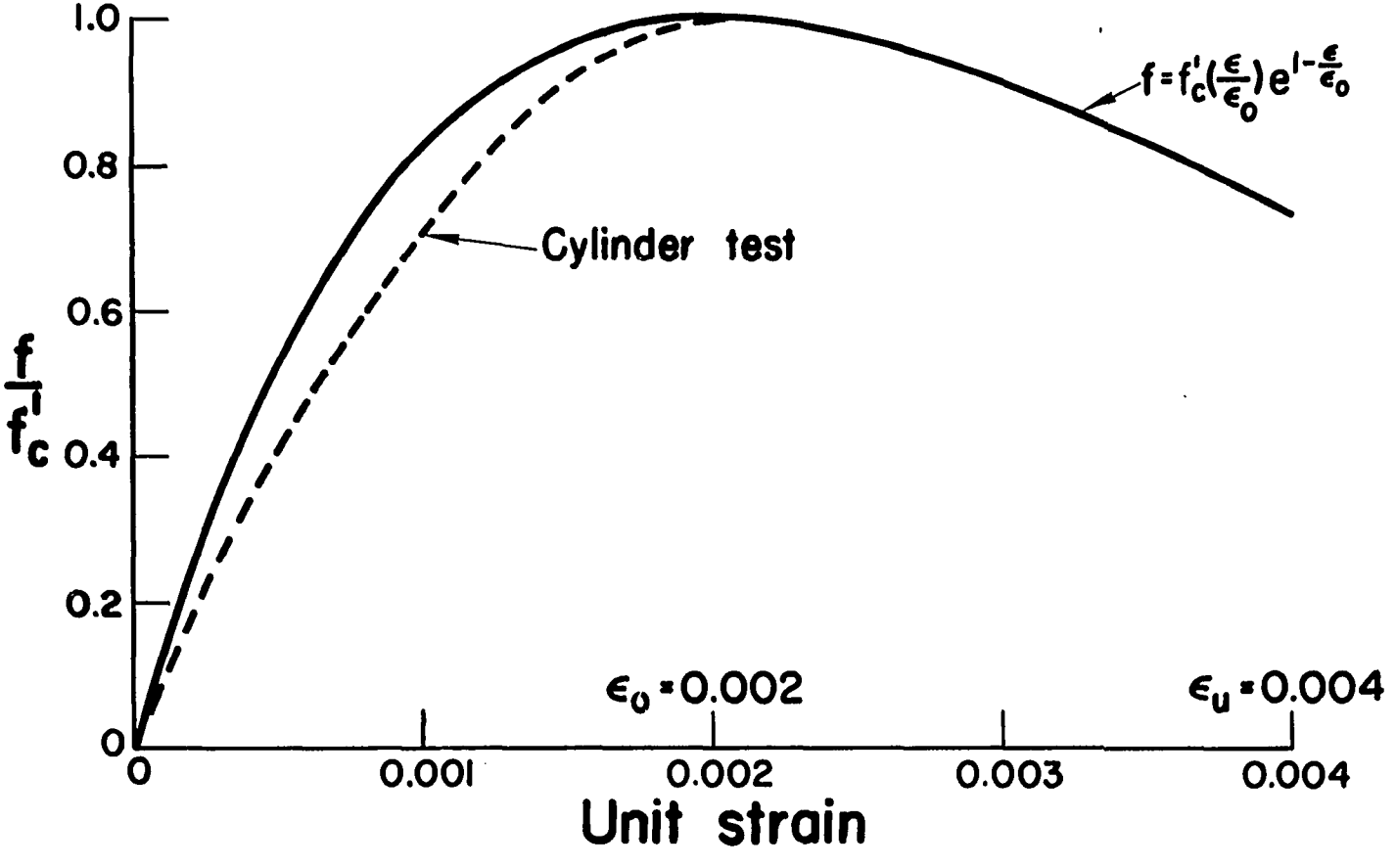

Figure 4. Comparison of stress-strain function with cylinder test

Figure 5. Distribution of normal stress and strain at a cross section

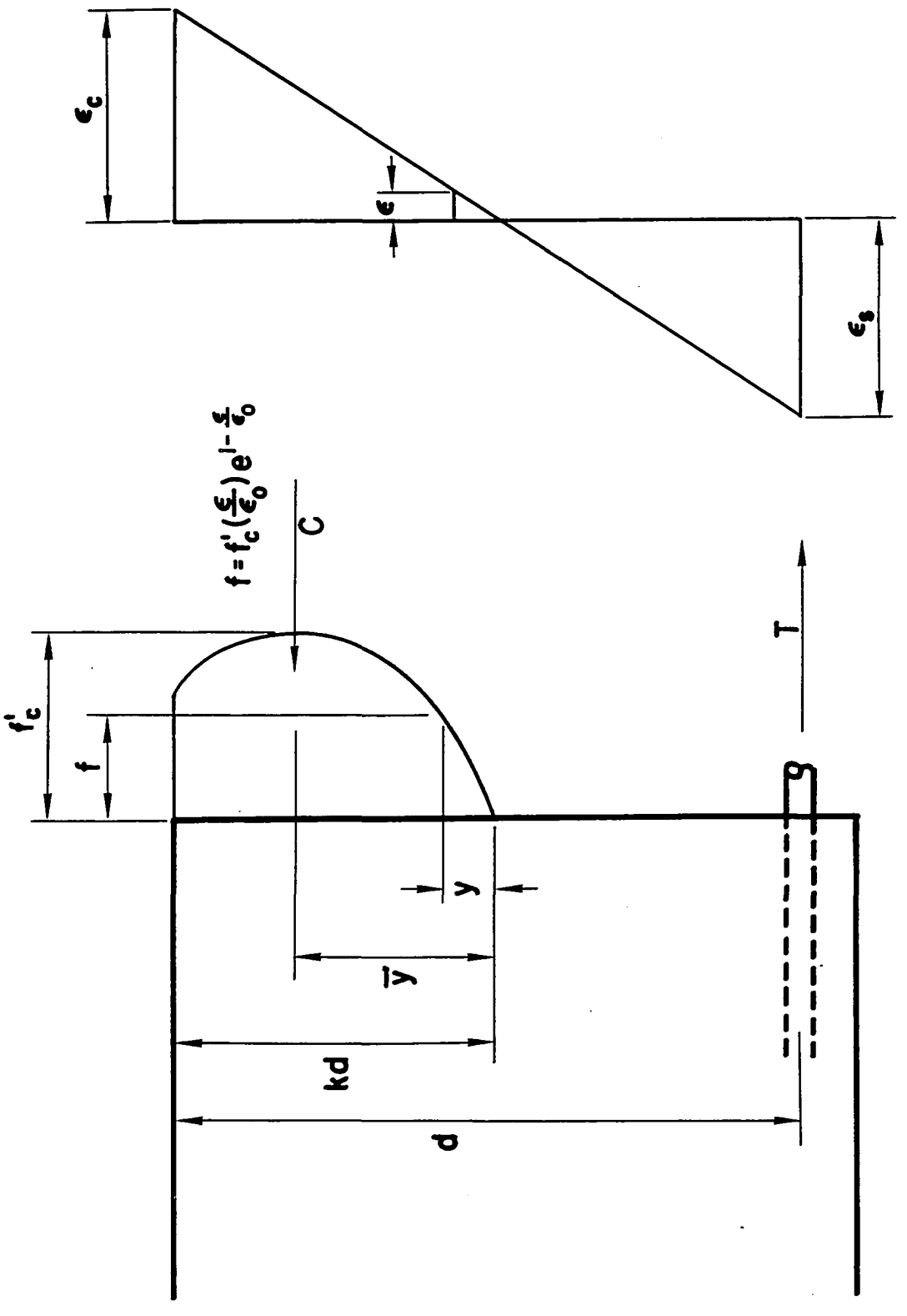
ϵ_c
ϵ
ϵ_s
$f = f'_c(\frac{\epsilon}{\epsilon_o})e^{1-\frac{\epsilon}{\epsilon_o}}$
C
T
f'_c
f
y
$\bar{y}$
kd
d

may be solved for ϵ_{cy}. Then

$$k_y d = \frac{\epsilon_{cy}}{\epsilon_{sy} + \epsilon_{cy}} d \tag{3}$$

The resultant compressive force, in general, may be located as follows:

$$\bar{y} = \frac{b\int_0^{kd} f\, y\, dy}{C} = \frac{\dfrac{b\, d^2\, f'_c}{\epsilon_o(\epsilon_s + \epsilon_c)^2} \displaystyle\int_0^{\epsilon_c} \epsilon^2\, e^{1 - \frac{\epsilon}{\epsilon_o}}\, d\epsilon}{\dfrac{bd\, f'_c}{\epsilon_o(\epsilon_s + \epsilon_c)} \displaystyle\int_0^{\epsilon_c} \epsilon\, e^{1 - \frac{\epsilon}{\epsilon_o}}\, d\epsilon}$$

Integrating and simplifying give

$$\bar{y} = \frac{d}{\epsilon_s + \epsilon_c}\left[2\epsilon_o - \frac{\epsilon_c^2\, e^{-\frac{\epsilon_c}{\epsilon_o}}}{\epsilon_o - (\epsilon_c + \epsilon_o)e^{-\frac{\epsilon_c}{\epsilon_o}}}\right] \tag{4}$$

At yield

$$\bar{y}_y = \frac{d}{\epsilon_{sy} + \epsilon_{cy}} \left[2\epsilon_o - \frac{\epsilon_{cy}^2 \, e^{-\frac{\epsilon_{cy}}{\epsilon_o}}}{\epsilon_o - (\epsilon_{cy} + \epsilon_o) \, e^{-\frac{\epsilon_{cy}}{\epsilon_o}}} \right] \quad (5)$$

Then, it is apparent that

$$M_y = C_y \, (d - k_y d + \bar{y}_y) \quad (6)$$

The shear at yield is

$$V_y = \frac{M_y}{L}$$

In analyzing the beams for shear, it was assumed that the entire shear at a cross section is carried by that concrete area which is in compression. Additionally, it was assumed that the shearing stress distribution can be expressed by a function similar to that of the normal stress, that is,

$$v = v_c' \left(\frac{\gamma}{\gamma_o}\right) e^{1 - \frac{\gamma}{\gamma_o}} \quad (7)$$

The ranges on the shear stress distribution are parabolic (for a linear distribution of normal stress) and linear (for a uniform distribution of normal stress). The assumed distribution of shear stress closely approximates that required by considerations of equilibrium.

The modulus of rigidity was taken as forty per cent of the modulus of elasticity, in accordance with tests reported by Zia (11). On the basis of tests with high triaxial stress performed by Balmer (12), the shearing strength of the concrete was assumed to be sixteen per cent of the compressive strength.

Differentiating Equation 1 gives

$$\frac{df}{d\epsilon} = \frac{f'_c}{\epsilon_o} e^{1 - \frac{\epsilon}{\epsilon_o}} \left(1 - \frac{\epsilon}{\epsilon_o}\right)$$

At $\epsilon = 0$

$$\frac{df}{d\epsilon} = \frac{f'_c}{\epsilon_o} e = E_c$$

and $$\epsilon_o = \frac{f'_c e}{E_c}$$

Similarly:

$$\gamma_o = \frac{v'_c e}{G_c}$$

But $v'_c = 0.16\, f'_c$

and $G_c = 0.40\, E_c$

so that

$$\gamma_o = \frac{0.16\, f'_c e}{0.40\, E_c} = 0.4\, \epsilon_o = 0.0008$$

Then, considering Figure 6,

$$V = b\int_0^{kd} v\, ds$$

where $\frac{\gamma}{s} = \frac{\gamma_{kd}}{kd}$ and $ds = \frac{kd}{\gamma_{kd}}\, d\gamma$

Then $V = \frac{b\, kd}{\gamma_{kd}} \int_0^{\gamma_{kd}} v\, d\gamma$

Substituting v from Equation 7, integrating between limits, and simplifying give

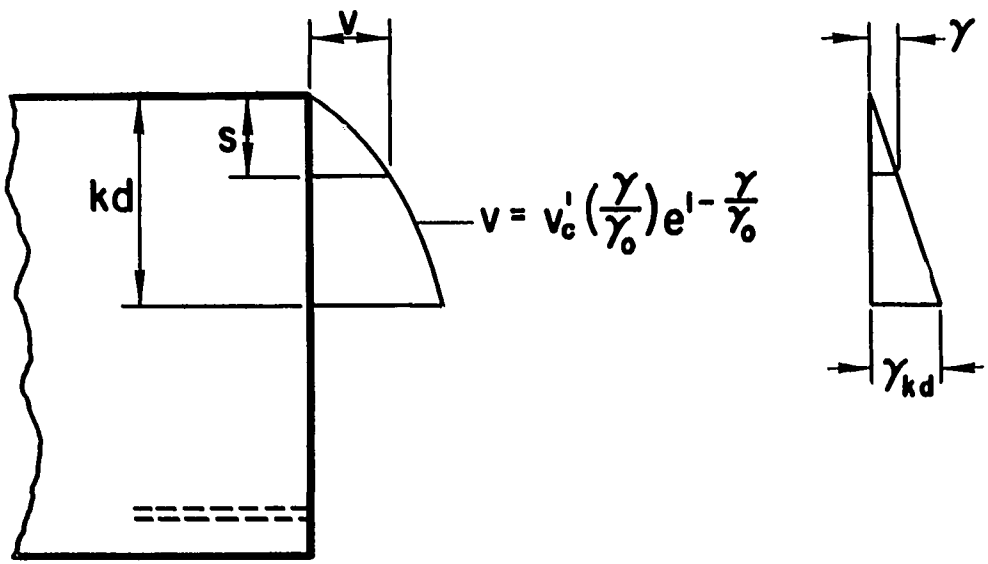

Figure 6. Distribution of shearing stress and strain at a cross section

$$V = \frac{b\ kd\ v'_c}{\gamma_{kd}} \left[(\gamma_o + \gamma_{kd})(-e^{1 - \frac{\gamma_{kd}}{\gamma_o}}) + \gamma_o e \right] \qquad (8)$$

When, at yield conditions, $kd = k_y d$

$$V_y = \frac{b\ k_y d\ v'_c}{\gamma_{k_y d}} \left[(\gamma_o + \gamma_{k_y d})(-e^{1 - \frac{\gamma_{k_y d}}{\gamma_o}}) + \gamma_o e \right] \qquad (9)$$

With $\gamma_o = 0.0008$ and $v'_c = 0.16\ f'_c$, Equation 9 may be solved for $\gamma_{k_y d}$.

Strain Energy at Yield Load

Timoshenko and Goodier (30) have shown that the strain energy per unit volume is

$$u = \frac{1}{2} \left[f_x \epsilon_x + f_y \epsilon_y + f_z \epsilon_z + v_{xy} \gamma_{xy} + v_{yz} \gamma_{yz} + v_{xz} \gamma_{xz} \right]$$

if forces on a body increase simultaneously in the same ratio. The strain energy for the beams of this investigation was summed part by part.

In considering first the reinforcing steel of area A_s, the x-axis is taken along the length of the beam with the origin at the support. All the shearing stresses and the normal stresses f_y and f_z were taken to be zero so that

the strain energy was

$$d\,U_s = \frac{1}{2} f_s\, \epsilon_s\, dx\, dy\, dz$$

But $\epsilon_s = \frac{f_s}{E_s}$ and $f_s = \frac{x}{L} f_{sy}$

So that

$$U_s = \frac{A_s}{2E_s} \int_0^L (\frac{x}{L}\ f_{sy})^2\, dx$$

Then the total strain energy in the reinforcing steel (on one-half of the beam) is

$$U_s = \frac{1}{6} \frac{f_{sy}^2}{E_s} A_s L \qquad (10)$$

It is seen that up to yield stress the strain energy in the longitudinal steel will vary as the square of the stress in the steel. This distribution of strain energy is shown in Figure 7.

Due to the normal stress in the concrete, the strain energy per unit volume, from Figure 5, is

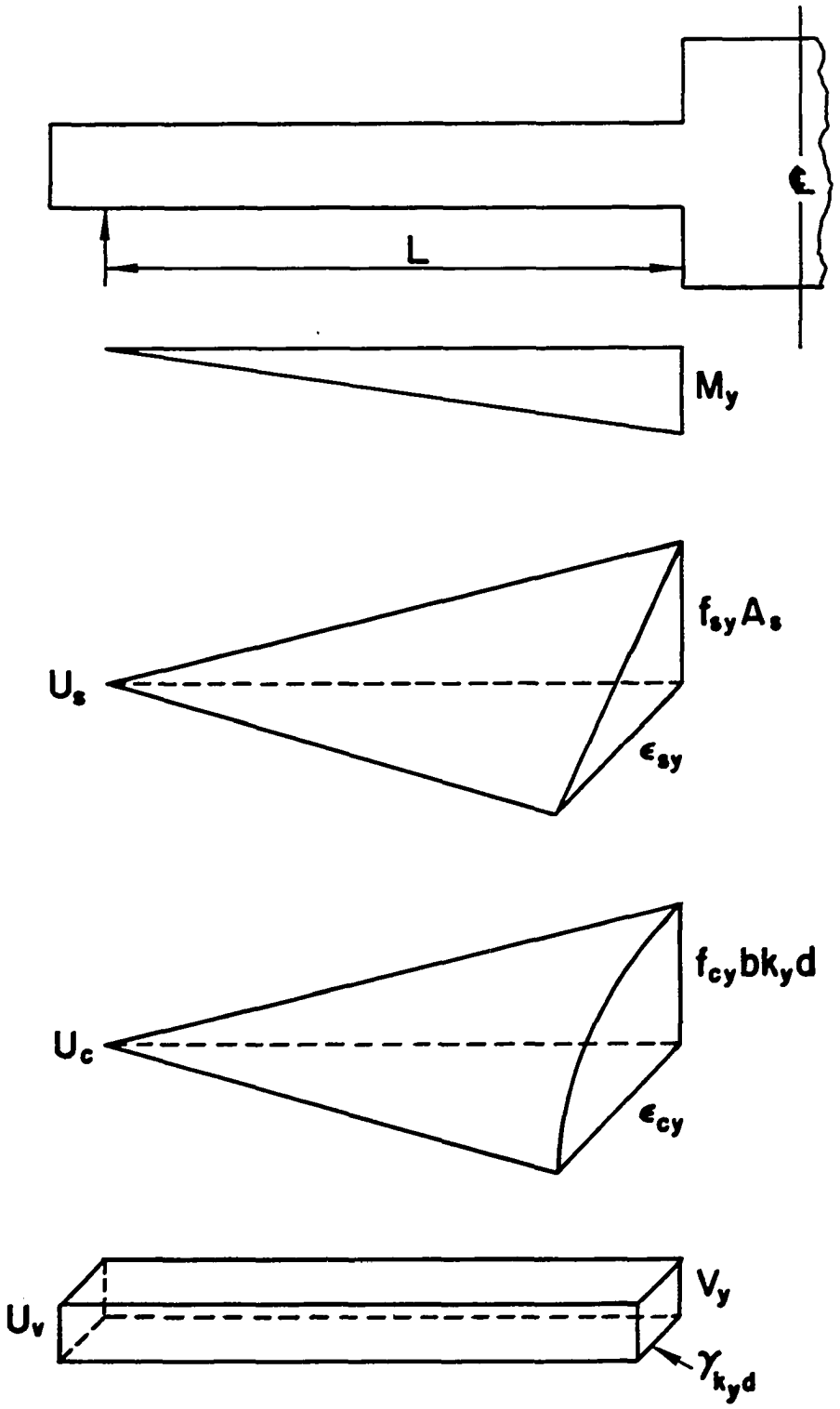

Figure 7. Distribution of strain energy at yield load

$$u_c = \int_0^{\epsilon_{cy}} f \, d\epsilon$$

Substituting f from Equation 1, integrating between limits, and simplifying give

$$u_c = f'_c \left[(\epsilon_o + \epsilon_{cy})(-e^{1 - \frac{\epsilon_{cy}}{\epsilon_o}}) + \epsilon_o e \right] \qquad (11)$$

It is assumed that the depth of the neutral axis remains the same for all sections from the face of the column stub to the support. It will be recognized that this is in error if the fact is considered that the beam has cross sections near the column face which are cracked and ones in the vicinity of the support which are uncracked. However, it is believed that the effect on the total strain energy is small enough so as not to warrant consideration of the uncracked section.

The distribution of strain energy due to normal stress in the concrete is shown in Figure 7. Then the strain energy (on one-half of the beam) is

$$U_c = \frac{1}{3} u_c \, b \, k_y d \, L \qquad (12)$$

But, combining $\frac{\epsilon_{cy}}{k_y d} = \frac{\epsilon_{cy} + \epsilon_{sy}}{d}$ with Equations 2, 11, and

12, there is obtained

$$U_c = \frac{1}{3} C_y \varepsilon_{cy} L \tag{13}$$

The strain energy due to shearing stress in the concrete may be determined in a manner similar to that for the normal stress. The strain energy per unit volume, from Figure 6, is

$$u_v = \int_0^{\gamma_{k_y d}} v \, d\gamma$$

Substituting v from Equation 7, integrating between limits, and simplifying give

$$u_v = v'_c \left[(\gamma_o + \gamma_{k_y d})(-e^{1 - \frac{\gamma_{k_y d}}{\gamma_o}}) + \gamma_o e \right] \tag{14}$$

The shearing force and shearing strain are constant over the length of the beam. Therefore, the strain energy (on one-half of the beam) is

$$U_v = u_v \, b \, k_y d \, L \tag{15}$$

Combining Equations 9, 14, and 15 gives

$$U_v = V_y \gamma_{k_y d} L \tag{16}$$

The total strain energy at yield is then

$$U_T = U_s + U_c + U_v \tag{17}$$

Conditions at Ultimate Load

In analyzing the beams at ultimate load, it was assumed that the unit strain in the concrete outer fiber was 0.004 at failure. Strains measured during the tests are given in Table 5. Values near these have been observed by Hognestad (14) and others. Equating forces normal to the cross section:

$$C_u = T_u = f_{su} A_s$$

Since all the equations leading to Equation 2 are general and valid to ultimate, the ultimate compressive force is

$$C_u = f_{su} A_s$$

$$= \frac{b\, d\, f'_c}{\epsilon_{su} + \epsilon_{cu}} \left[(\epsilon_o + \epsilon_{cu})\left(-e^{1 - \frac{\epsilon_{cu}}{\epsilon_o}}\right) + \epsilon_o e \right] \tag{2A}$$

Table 5. Unit strains and testing times

Beam	ϵ_{cu}[a]	$\epsilon_{su(test)}$[a]	$\epsilon_{su(calc.)}$	Testing time[b]
8-1-A	0.0046	0.0280+[c]	0.027	30.6
8-1-B	0.0045	0.0232	0.022	31.3
8-1-C	0.0045	0.0230+	0.027	30.6
8-2-A	0.0031	0.0249	0.017	20.0
8-2-B	0.0031	0.0161	0.012	21.4
8-2-C	0.0040	0.0188	0.012	19.7
8-3-A	0.0040	0.0113+	0.010	16.2
8-3-B	0.0048	0.0175	0.007	15.7
8-3-C	0.0041	0.0115	0.010	17.7
6-1-A	0.0046	0.0268	0.022	18.5
6-1-B	0.0018	0.0223+	0.027	21.2
6-1-C	0.0046	0.0174	0.027	17.6
6-2-A	0.0058	0.0209	0.012	19.7
6-2-B	0.0050	0.0212	0.011	10.8
6-2-C	0.0059	0.0225	0.012	18.2
6-3-A	0.0040	0.0145	0.011	11.8
6-3-B	0.0054	0.0019	0.007	17.3
6-3-C	0.0050	0.0145	0.010	11.9
4-1-A	0.0058	0.0222	0.021	18.7
4-1-B	0.0040	0.0297+	0.027	16.9
4-1-C	0.0038	0.0282	0.027	12.7
4-2-A	0.0036	0.0210	0.012	14.8
4-2-B	0.0039	0.0202	0.017	11.5
4-2-C	0.0040	0.0310+	0.018	16.8
4-3-A	0.0041	0.0230	0.010	11.6
4-3-B	0.0034	0.0073	0.010	8.8
4-3-C	0.0044	0.0014	0.011	6.0

[a]These are maximum observed values.

[b]To reach ultimate load (minutes).

[c]Plus sign indicates SR-4 gage failed before ultimate load was reached.

But

$$\left[(\epsilon_o + \epsilon_{cu})(-e^{1-\frac{\epsilon_{cu}}{\epsilon_o}}) + \epsilon_o e\right] = 0.00323$$

since $\epsilon_o = 0.002$ and $\epsilon_{cu} = 0.004$ as shown in Figure 4. Then

$$f_{su} = \frac{b\ d\ f'_c}{A_s(\epsilon_{su} + \epsilon_{cu})}\ (0.00323) \qquad (18)$$

The unit stress and unit strain in the steel may be determined by considering the stress-strain curve for the material (see Figure 1) in addition to Equation 18. Then

$$k_u d = \frac{\epsilon_{cu}}{\epsilon_{su} + \epsilon_{cu}}\ d$$

Then the moment at ultimate load, from Figure 5, is

$$M_u = f_{su}\ A_s \left[d - k_u d + \bar{y}_u\right]$$

But from Equation 4

$$\frac{\bar{y}_u}{k_u d} = \frac{1}{\epsilon_{cu}}\left[2\epsilon_o - \frac{\epsilon_{cu}^2\ e^{-\frac{\epsilon_{cu}}{\epsilon_o}}}{\epsilon_o - (\epsilon_{cu} + \epsilon_o)\ e^{-\frac{\epsilon_{cu}}{\epsilon_o}}}\right]$$

and setting $\epsilon_o = 0.002$ and $\epsilon_{cu} = 0.004$ then

$$\frac{\bar{y}_u}{k_u d} = 0.544$$

so that

$$M_u = f_{su} A_s \left[d - 0.456\, k_u d\right]$$

The shear at ultimate load is

$$V_u = \frac{M_u}{L}$$

The shearing strain at ultimate load may be determined from Equation 8 since it is also valid at ultimate. This gives

$$V_u = \frac{b\, k_u d\, v_c'}{\gamma_{k_u d}} \left[(\gamma_o + \gamma_{k_u d})(-e^{1 - \frac{\gamma_{k_u d}}{\gamma_o}}) + \gamma_o e\right] \qquad (19)$$

Strain Energy at Ultimate Load

Plasticity in both steel and concrete is shown in Figure 8 to extend a distance m from the face of the column.

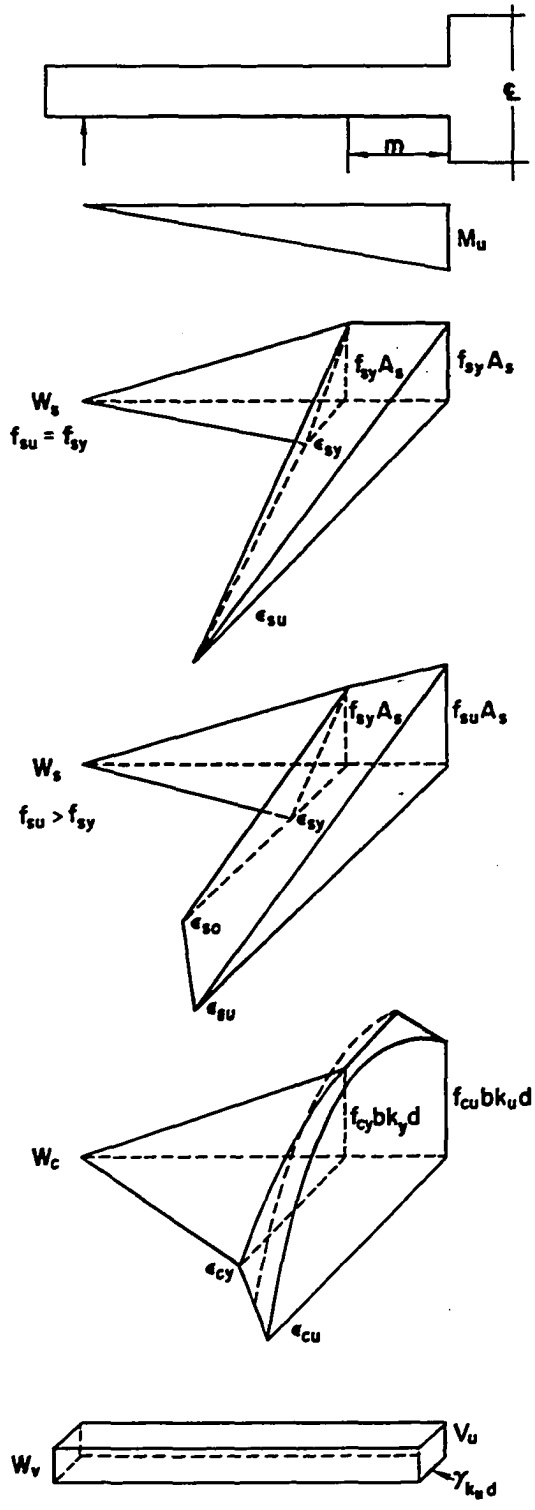

Figure 8. Distribution of strain energy at ultimate load

Two cases are given for the strain energy in the reinforcing steel: the first in which the unit stress at ultimate load is equal to the yield stress and a second in which the unit stress at ultimate load is greater than the yield stress. A special case must be made for beams 8-1-A and C, beams 6-1-B and C, and beams 4-1-B and C. For these beams the yield stress is taken to be 42.5 ksi and the strain energy is evaluated from the first diagram with the unit stress at the face of the column equal to f_{su} greater than f_{sy}.

The total strain energy, W, on one-half of the beam is equal to the sum of the volumes of the appropriate diagrams. For the case in which $f_{su} = f_{sy}$

$$W_s = \frac{1}{6} f_{sy} A_s \epsilon_{sy} L + \frac{1}{6} f_{sy} A_s \epsilon_{su} m$$

$$+ \frac{1}{6} f_{sy} A_s \left[\sqrt{\epsilon_{sy}\epsilon_{su}}\right] m$$

For f_{su} greater than f_{sy}

$$W_s = \frac{1}{6} f_{sy} A_s \epsilon_{sy} \left[L-m\right]$$

$$+ \frac{1}{6} \left[f_{sy}\epsilon_{so} + f_{su}\epsilon_{su} + \sqrt{f_{sy}\epsilon_{so} f_{su}\epsilon_{su}}\right] A_s m$$

The strain energy due to normal stress on the concrete

is

$$W_c = \frac{1}{3} b k_y d f'_c \left[L - m\right] \left[(\varepsilon_o + \varepsilon_{cy})(-e^{1 - \frac{\varepsilon_{cy}}{\varepsilon_o}}) + \varepsilon_o e\right]$$

$$+ \frac{1}{6} b f'_c m \left[w_1 + 4w_2 + w_3\right]$$

where

$$w_1 = k_y d \left[(\varepsilon_o + \varepsilon_{cy})(-e^{1 - \frac{\varepsilon_{cy}}{\varepsilon_o}}) + \varepsilon_o e\right]$$

$$w_2 = \frac{1}{2} \left[k_y d + k_u d\right]$$

$$\left[(\varepsilon_o + \frac{\varepsilon_{cy} + \varepsilon_{cu}}{2})(-e^{1 - \frac{\varepsilon_{cy} + \varepsilon_{cu}}{2\,\varepsilon_o}}) + \varepsilon_o e\right]$$

$$w_3 = k_u d \left[(\varepsilon_o + \varepsilon_{cu})(-e^{1 - \frac{\varepsilon_{cu}}{\varepsilon_o}}) + \varepsilon_o e\right]$$

This may be simplified to

$$W_c = \frac{1}{3} C_y \varepsilon_{cy} L - \frac{1}{6} C_y \varepsilon_{cy} m$$

$$+ \frac{1}{3} b f'_c m \left[k_y d + k_u d\right]$$

$$\left[(\epsilon_o + \frac{\epsilon_{cy} + \epsilon_{cu}}{2\epsilon_o})(-e^{1 - \frac{\epsilon_{cy} + \epsilon_{cu}}{2\epsilon_o}}) + \epsilon_o e\right]$$

$$+ \frac{1}{6} b f'_c m k_u d \, [0.00323]$$

Since all the equations leading to Equation 16 are general and may be extended to the ultimate load, the strain energy due to shear at ultimate is

$$W_v = V_u \gamma_{k_u d} L \qquad (16A)$$

The total strain energy at ultimate is then

$$W_T = W_s + W_c + W_v \qquad (20)$$

The length m which is subject to plasticity is a factor of importance in determining the amount of strain energy in a beam at ultimate load. This length depends to some extent upon the shape of the external bending moment diagram. For the beams of this investigation, this influence may be reflected in the ratio of the ultimate moment to the yield moment. Tests results (5) have shown that the spread of plasticity depends on the unit strain in the longitudinal reinforcement and the percentage of reinforcement. The length

of plasticity was also assumed to be a function of the beam depth. Thus, the length of beam subject to plasticity could be expressed as follows:

$$m = F_1(p, d, \frac{M_u}{M_y}, \epsilon_{su})$$

The following equations of dimensionless terms could then be written:

$$\frac{m}{d} = F_2(p, \frac{M_u}{M_y}, \epsilon_{su})$$

Information regarding the manner in which the dimensionless terms combine could be obtained if the three terms on the right side of the equation could successively be kept constant in pairs while varying the third term. That was not possible in this investigation. Accordingly, it was assumed that the function combined by multiplication, giving

$$\frac{m\ M_y}{pdM_u} = A\epsilon_{su}$$

The constant A was evaluated by use of Figure 9. Then, the length of plasticity is

Figure 9. Length of beam subject to plasticity

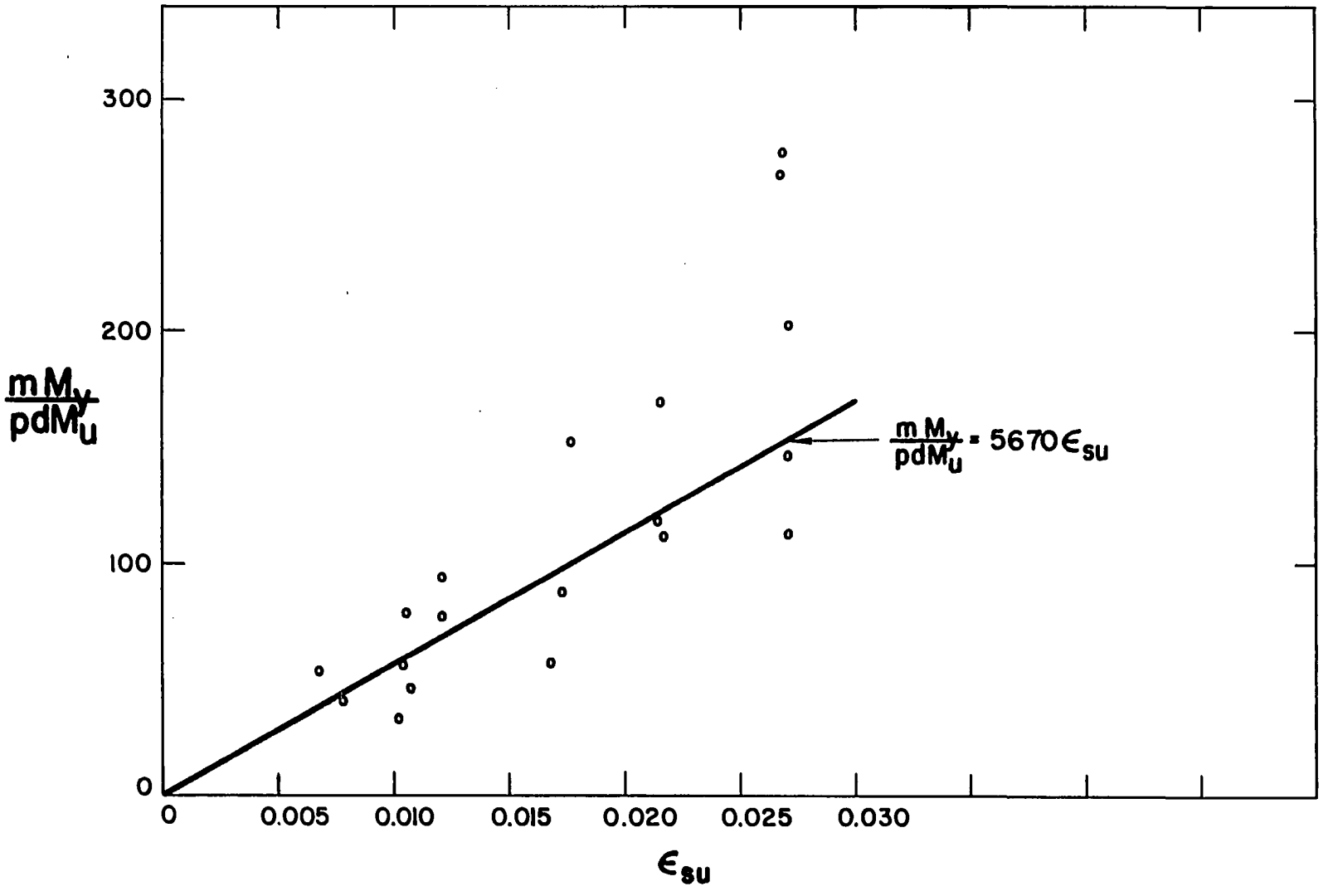
300
200
100
0
0
0.005
0.010
0.015
0.020
0.025
0.030
$\frac{m M_y}{pdM_u}$
$\frac{m M_y}{pdM_u} = 5670 \epsilon_{su}$
ϵ_{su}

$$m = 5670\ \epsilon_{su}\ p\ d\ \frac{M_u}{M_y} \qquad (21)$$

The values of m in the ordinates $\frac{m\ M_y}{pdM_u}$ in Figure 9 were determined by equating the total strain energy at ultimate load to the external work at ultimate load. The external work was evaluated as the area under the load-deflection curves, Figure 10. The yield and ultimate moments were those determined theoretically. The total strain energy at ultimate load for all the beams was then calculated using lengths of plasticity as found from Equation 21.

Deflections and Rotations

The deflections of the beams at yield load may be computed by equating the external work to the strain energy as determined from Equation 17:

$$\frac{1}{2}\ V_y\ \Delta_y = U_T$$

where $V_y = \frac{M_y}{L}$. Then

$$\Delta_y = \frac{2U_T}{V_y} \qquad (22)$$

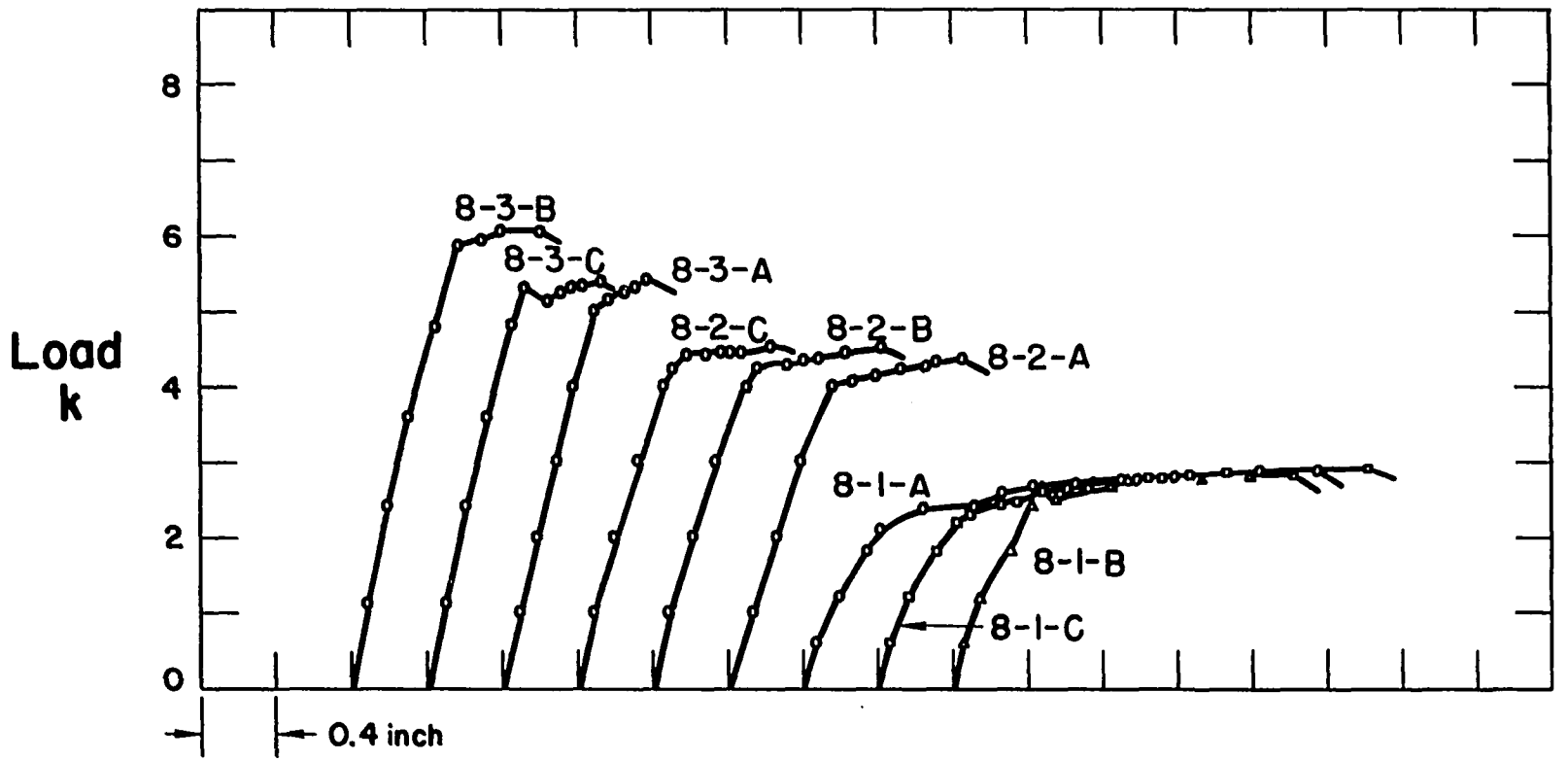

Figure 10. Load-deflection curves

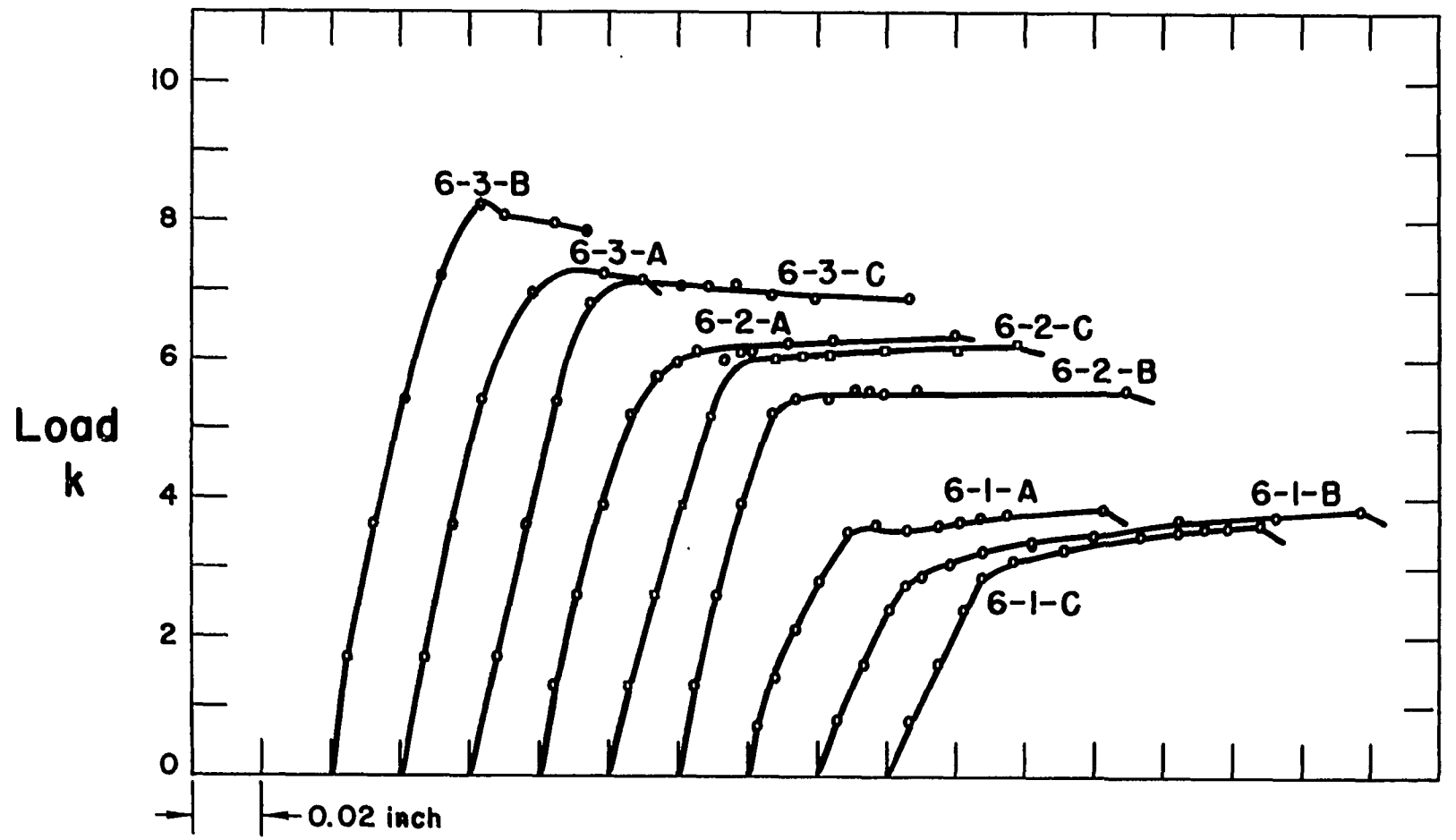

Figure 10. (Continued)

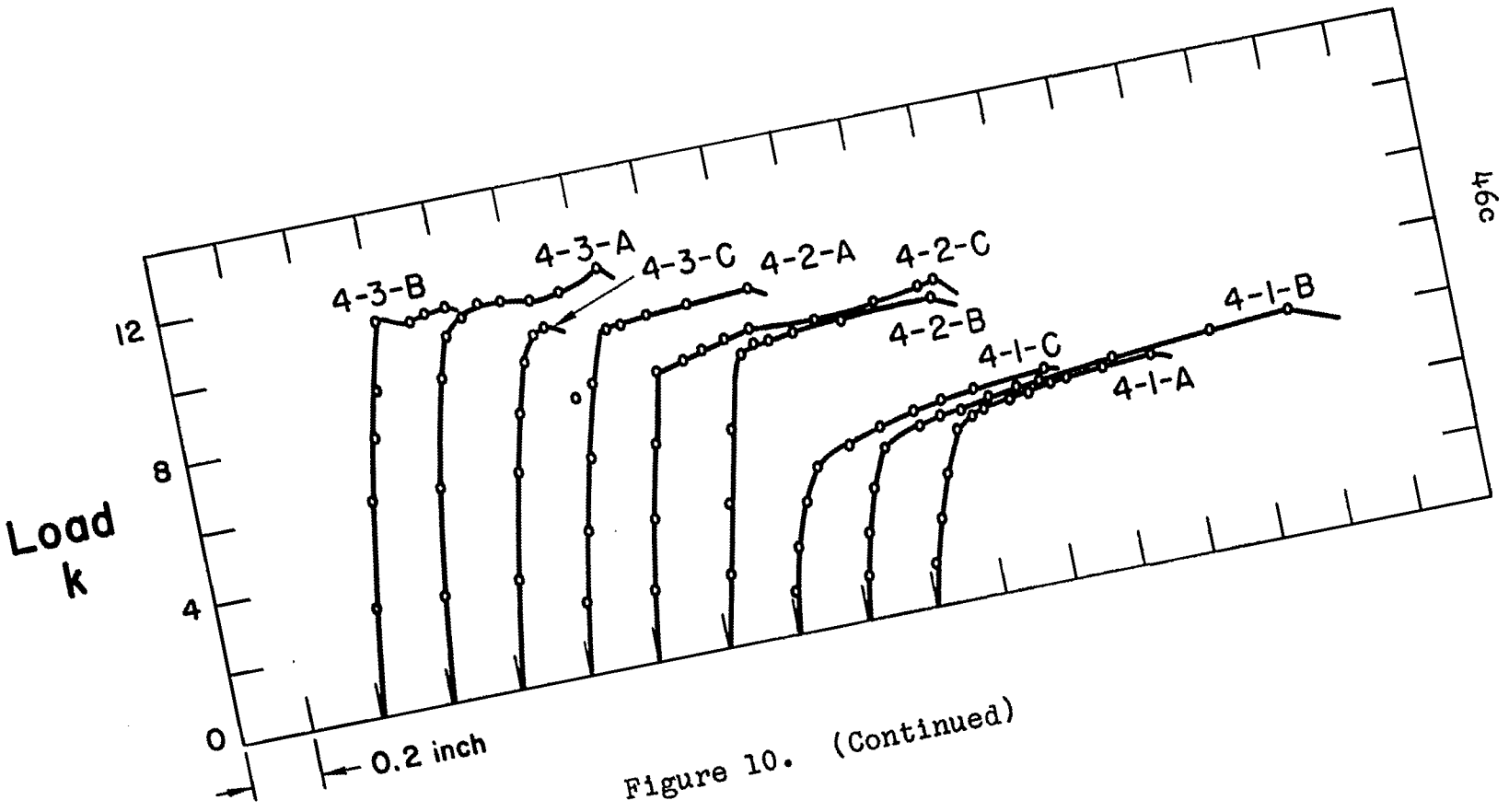

Figure 10. (Continued)

Similarly, the deflections at ultimate load can be computed by equating the external work at ultimate load to the strain energy W_T from Equation 20.

$$\frac{1}{2} V_y \Delta_y + \frac{1}{2} (V_y + V_u)(\Delta_u - \Delta_y) = W_T$$

and

$$\Delta_u = \frac{2 W_T + V_u \Delta_y}{V_y + V_u} \tag{23}$$

The plastic rotation θ_p, which is assumed to be concentrated at the face of the column, is

$$\theta_p = \frac{\Delta_u - \Delta_y}{L} \tag{24}$$

TEST RESULTS

Modes of Failure

All beams failed in flexure except 4-3-B and 4-3-C which failed in shear-compression. In a typical flexure failure, the tension reinforcement yielded. After yielding, the neutral axis shifted upward causing a reduction of the area of concrete in compression until, finally, the concrete ruptured. The shear-compression failure occurred when the intrusion of a diagonal crack into the compression area so reduced that area that the concrete crushed.

The cracks in the beams at which large rotations occurred were nearly all vertical. As the effect of shear became larger, with decreasing ratio of moment to shear, small inclined cracks appeared. The openings at these inclined cracks were too small to measure (Figure 11).

Loads

Photographs were taken of the beams at intervals throughout the test, including at the yield and ultimate loads. The yield load of a beam was detected by noting the halting of the load-indicating dial of the testing machine. This load in many cases was slightly higher than the load at

which yielding of the tensile reinforcement was first observed. Beyond the ultimate deflection the beams failed to increase in load-carrying capacity.

Theoretical values of yield and ultimate loads are compared with test values in Table 6.

Measurements

The measurements of unit strain at the outer fiber of the concrete indicated that values greater than 0.004 existed in many of the beams, in one case as far as 2-1/2 inches from the face of the column. Values of unit strain are given in Table 5. These values are not the absolute maximum unit strains which existed in the beams but are lower limits of them. For computation purposes, a maximum unit strain of 0.004 was assumed in the beam region subject to plasticity. The strain measurements at the outer fiber are not a good indication of the extent of spread of plasticity because in most instances the piece of concrete to which the gages were attached would break out to a depth of 1/2 inch to 1 inch and to varying lengths. An example of this is shown in Figure 11. In these cases, the maximum unit strain probably occurs between the outer fiber and the neutral axis.

The calculated unit strains at ultimate in the reinforcing were lower in most cases than the measured values.

Table 6. Yield and ultimate loads

Beam	$V_{y(calc.)}$ k	$V_{y(test)}$ k	$\frac{V_{y(test)}}{V_{y(calc.)}}$	$V_{u(calc.)}$ k	$V_{u(test)}$ k	$\frac{V_{u(test)}}{V_{u(calc.)}}$
8-1-A	1.06	1.04	0.98	1.47	1.43	0.97
8-1-B	1.28	1.30	1.02	1.46	1.42	0.97
8-1-C	1.07	1.15	1.07	1.48	1.45	0.98
8-2-A	1.93	2.00	1.04	2.06	2.18	1.06
8-2-B	2.11	2.12	1.00	2.17	2.25	1.04
8-2-C	2.11	2.13	1.01	2.17	2.26	1.04
8-3-A	2.74	2.50	0.91	2.84	2.70	0.95
8-3-B	2.97	2.94	0.99	3.00	3.03	1.01
8-3-C	2.74	2.65	0.97	2.84	2.68	0.94
6-1-A	1.71	1.75	1.02	1.93	1.91	0.99
6-1-B	1.42	1.37	0.97	1.97	1.91	0.97
6-1-C	1.42	1.55	1.09	1.97	1.81	0.92
6-2-A	2.81	2.88	1.02	2.90	3.17	1.09
6-2-B	2.48	2.72	1.10	2.57	2.77	1.08
6-2-C	2.81	3.05	1.09	2.90	3.11	1.07
6-3-A	3.67	3.62	0.99	3.81	3.68	0.97
6-3-B	3.93	4.11	1.05	4.00	4.11	1.03
6-3-C	3.66	3.40	0.93	3.78	3.54	0.94
4-1-A	2.56	2.40	0.94	3.37	2.90	0.96
4-1-B	2.13	2.33	1.09	2.97	3.14	1.06
4-1-C	2.13	2.28	1.07	2.96	2.96	1.00

Table 6. (Continued)

Beam	$V_{y(calc.)}$ k	$V_{y(test)}$ k	$\frac{V_{y(test)}}{V_{y(calc.)}}$	$V_{u(calc.)}$ k	$V_{u(test)}$ k	$\frac{V_{u(test)}}{V_{u(calc.)}}$
4-2-A	4.22	4.71	1.12	4.35	4.87	1.12
4-2-B	3.86	4.11	1.06	4.16	4.29	1.03
4-2-C	3.90	4.03	1.03	4.26	4.51	1.06
4-3-A	5.50	5.43	0.99	5.69	5.60	0.98
4-3-B	5.58	5.45	0.98	5.75	5.47	0.95
4-3-C	5.51	----	----	5.71	----	----

One cause of this was the reduction of cross sectional area of the reinforcing as a result of filing off deformations. The calculated strains are believed to be more accurate.

Measurements of the rotation which occurred at a crack between zero load and the ultimate load were made directly from the photographic negative. A 1/2-inch grid was penciled on the white-washed surface of the beam to serve as points of reference. Readings of the crack opening were made at 1/2-inch intervals of the height of the beam on the picture corresponding to the ultimate load. Initial readings were obtained from the picture taken at zero load. A filar micrometer was used to make the measurements.

Determinations of the crack opening at yield load were not made. The size of these cracks at the bottom surface of the beam was about 0.006 inch (15) or near the limit of accuracy of the system. The size of the cracks at ultimate load was as large as 0.15 inch.

All of the measurements over the height of the beam at an individual crack were plotted on graph paper. From each graph were determined the rotation which occurred at the crack and the location of the neutral axis. The depths to the neutral axis are compared to those determined theoretically in Table 7. The test values of θ_p in Table 7 are the averages of the sums of the rotation occurring at cracks on each side of the column stubs; θ_p is a plastic

Figure 11. Test specimen

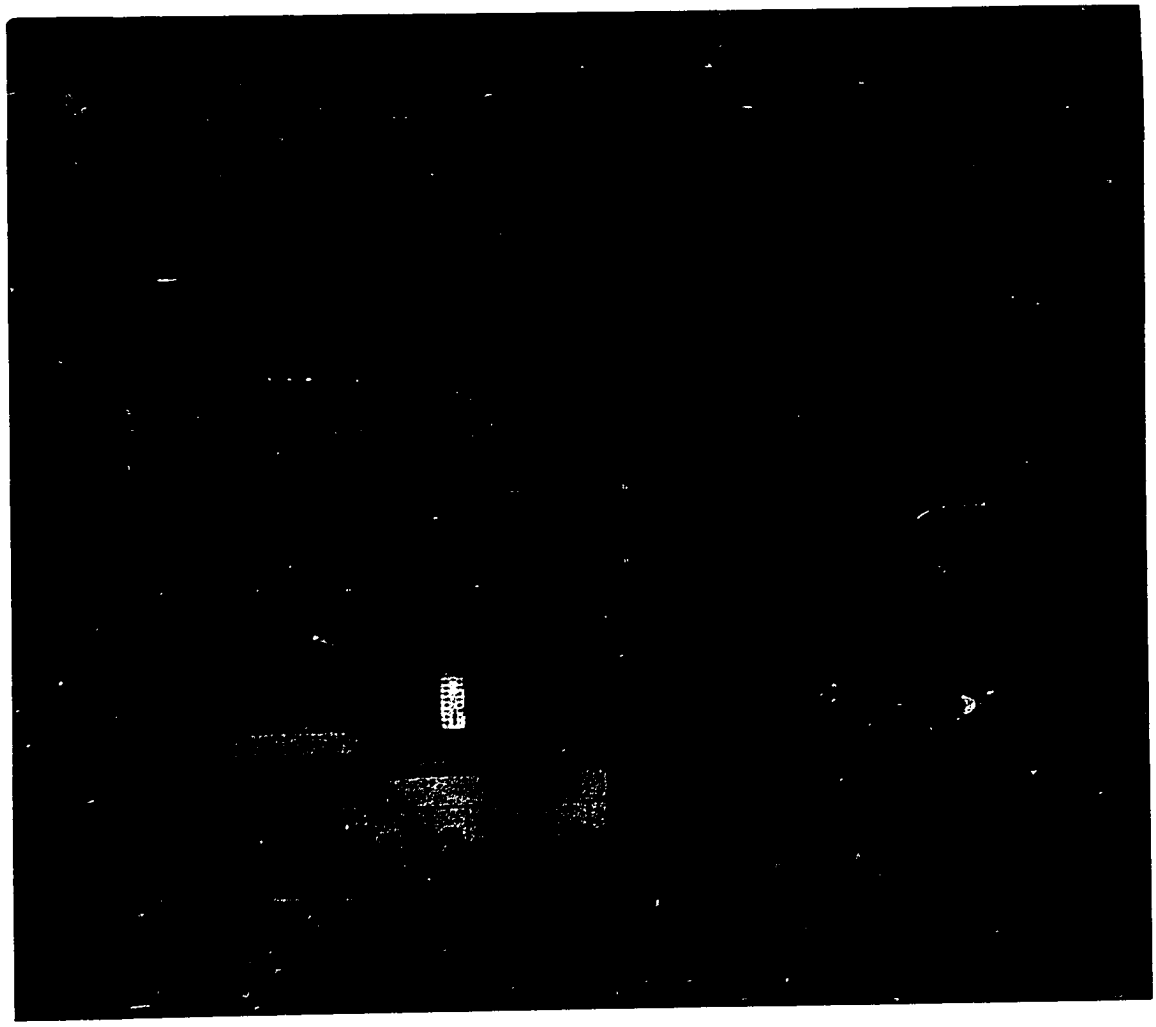

Figure 11. (Continued)

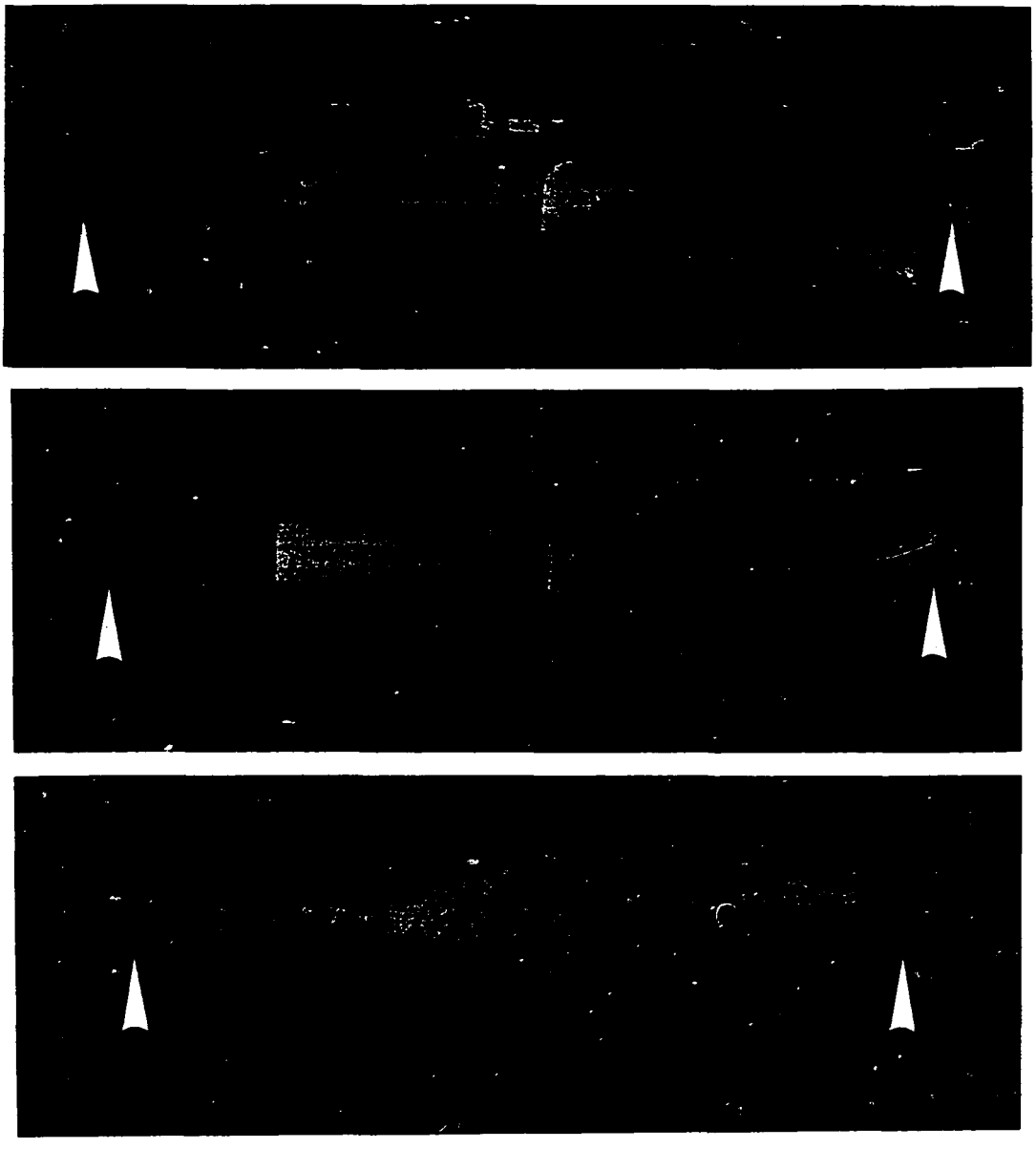

Table 7. θ_p and $k_u d$

Beam	$\theta_{p(test)}$ rad	$\theta_{p(calc.)}$ rad	$k_u d_{(test)}$ in.	$k_u d_{(calc.)}$ in.
8-1-A	0.0485	0.0156	1.60	0.82
8-1-B	0.0240	0.0190	1.06	0.98
8-1-C	0.0388	0.0228	1.15	0.82
8-2-A	0.0153	0.0250	1.31	1.20
8-2-B	0.0126	0.0092	1.34	1.56
8-2-C	0.0167	0.0085	1.71	1.56
8-3-A	0.0092	0.0116	1.80	1.73
8-3-B	0.0110	0.0065	1.86	2.29
8-3-C	0.0104	0.0041	1.55	1.73
6-1-A	0.0224	0.0252	1.12	0.98
6-1-B	0.0393	0.0246	1.02	0.81
6-1-C	0.0198	0.0246	1.14	0.81
6-2-A	0.0260	0.0101	1.34	1.56
6-2-B	0.0130	0.0082	1.50	1.65
6-2-C	0.0289	0.0080	1.80	1.56
6-3-A	0.0108	0.0052	1.55	1.68
6-3-B	------	0.0060	----	2.29
6-3-C	0.0103	0.0032	1.35	1.72
4-1-A	0.0312	0.0208	1.09	1.00
4-1-B	0.0504	0.0285	0.72	0.81
4-1-C	0.0349	0.0298	1.40	0.81
4-2-A	0.0223	0.0076	1.34	1.56
4-2-B	0.0246	0.0264	0.95	1.17
4-2-C	0.0376	0.0218	1.25	1.16
4-3-A	0.0219	0.0117	1.74	1.72
4-3-B	0.0131	------	1.31	1.73
4-3-C	------	------	----	1.68

rotation assumed to be concentrated at the face of the column.

Load-Deflection Curves

The deflection of the column stub with respect to the supports of the beam was obtained from the photographic negative by the indications of dial gages. The readings are plotted in the form of load-deflection curves in Figure 10. The values plotted are averages of those obtained at the north and south sides of the column stub.

The deflections determined theoretically at both yield and ultimate loads are compared with the test values in Table 8.

Plastic Rotations

The primary objective of this investigation was to determine the influence of combined bending moment and shear on the plastic rotation of reinforced concrete members. This influence is shown in Figure 12, where the plastic rotation θ_p is plotted against the ratio $\frac{M}{Vd}$. From the average values plotted, a decreasing trend in plastic rotation is observed with increasing $\frac{M}{Vd}$, but the data are insufficient for more definite conclusions.

Table 8. Deflections at yield and ultimate loads

Beam	$\Delta_{y(test)}$ in.	$\Delta_{y(calc.)}$ in.	$\Delta_{u(test)}$ in.	$\Delta_{u(calc.)}$ in.
8-1-A	0.41	0.40	2.75	1.19
8-1-B	0.46	0.52	1.82	1.48
8-1-C	0.48	0.40	2.60	1.55
8-2-A	0.56	0.51	1.25	1.76
8-2-B	0.59	0.65	1.23	1.11
8-2-C	0.50	0.65	1.04	1.07
8-3-A	0.51	0.61	0.93	1.18
8-3-B	0.57	0.74	1.00	1.06
8-3-C	0.52	0.61	0.92	0.81
6-1-A	0.29	0.31	1.05	1.26
6-1-B	0.25	0.23	1.57	1.17
6-1-C	0.28	0.23	0.98	1.17
6-2-A	0.34	0.38	1.22	0.76
6-2-B	0.34	0.36	1.30	0.66
6-2-C	0.36	0.38	1.16	0.68
6-3-A	0.31	0.35	0.70	0.54
6-3-B	0.43	0.44	0.72	0.66
6-3-C	0.34	0.36	0.76	0.47
4-1-A	0.15	0.15	0.73	0.68
4-1-B	0.14	0.11	1.34	1.34
4-1-C	0.14	0.11	0.83	0.86
4-2-A	0.23	0.21	0.65	0.40
4-2-B	0.23	0.15	0.75	0.81
4-2-C	0.23	0.15	0.97	0.69
4-3-A	0.27	0.18	0.62	0.47
4-3-B	----	----	0.39	----
4-3-C	----	----	0.26	----

Figure 12. Effect of shear span to depth ratio on plastic rotation

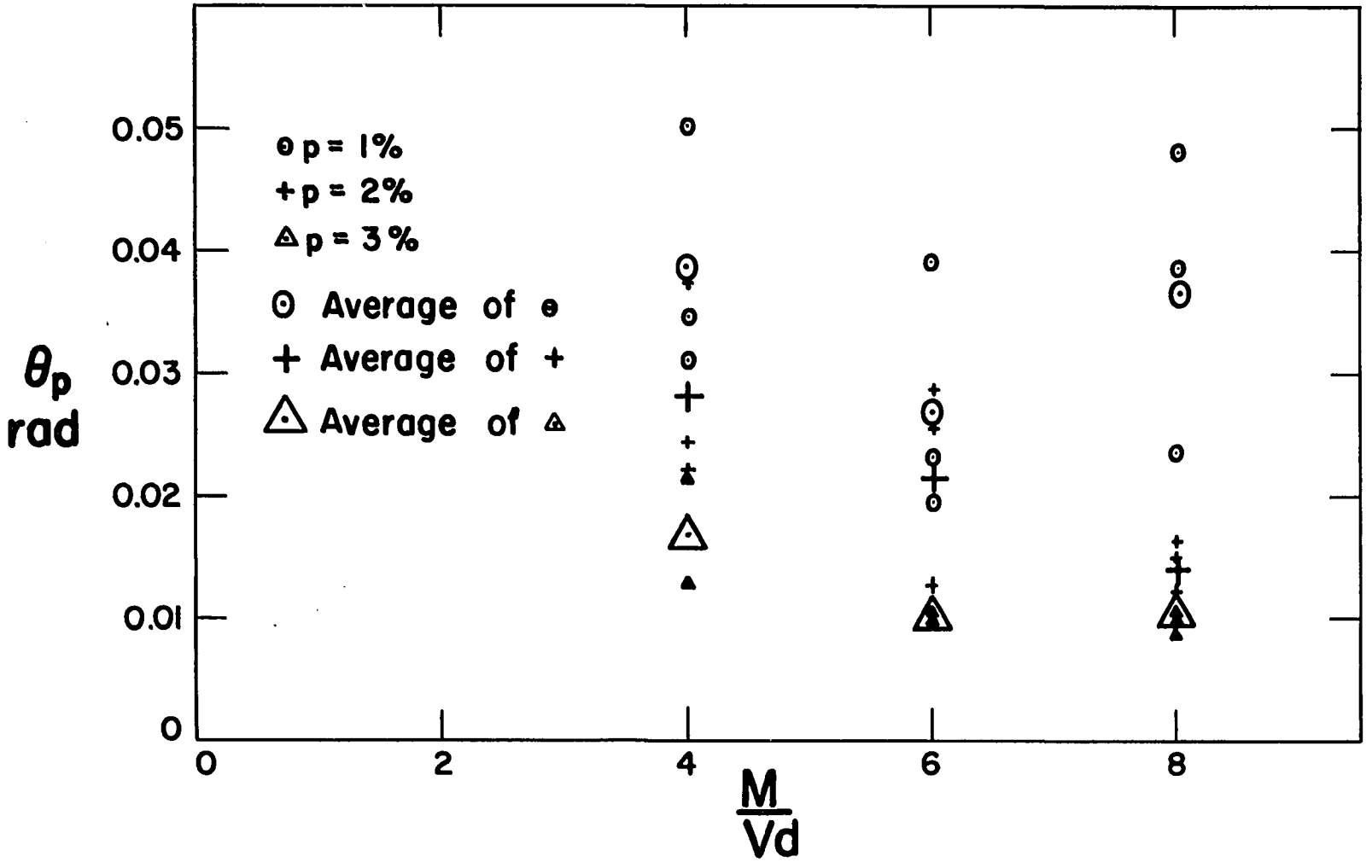
0.05
0.04
0.03
0.02
0.01
0
θ_p rad
o p = 1%
+ p = 2%
△ p = 3%
O Average of o
+ Average of +
△ Average of △
0
2
4
6
8
M/Vd

SUMMARY AND CONCLUSIONS

The deflections of the beams at yield load as determined by the principles of strain energy showed an average error of 15 per cent when compared to the measured deflections. The maximum error was 35 per cent. The comparison of measured deflections at ultimate load to the computed values showed an average error of 23 per cent and a maximum error of 58 per cent.

One possible cause of the lack of better agreement between measured and computed deflections at ultimate load might be the difficulty of discerning the ultimate load and the corresponding ultimate deflection. This would be particularly true with the beams of smallest percentage of reinforcement since they have flatter and longer load-deflection curves.

Another factor which influences the storing of strain energy is time. The attempt in this research to lessen the effect of time by testing all beams within the same duration did not meet with complete success. The more flexible beams required a greater time to reach ultimate load. They were therefore subject to greater amounts of creep, and it is quite likely that creep accounts for the difference between measured external work and calculated strain energy.

The amount of available plastic rotation decreases

with increasing ratio of shear span to depth, $\frac{M}{Vd}$.

It is contended in this report, contrary to the position held by others, that the extent of spread of plasticity increases with percentage of longitudinal reinforcement, all other factors being constant. If, among the quantities p, d, $\frac{M_u}{M_y}$, and ϵ_{su}, two beam cross sections are identical except for percentage of reinforcement, then that beam which has the larger percentage of reinforcement will have a greater spread of plasticity. This follows from the fact that the beam with larger percentage of reinforcement also has a larger compressive force on the concrete and a greater depth to the neutral axis, thus subjecting more material to plasticity.

It is believed that tests of simulated beam-column connections should have a device of some nature which applies axial load to the top and bottom of the column stub portion. This will approximate more closely the conditions met in service and will serve to prevent the opening of horizontal cracks through the column stub at the level of the reinforcement. These horizontal cracks facilitate greatly the spread of plasticity into the column by destroying bond stresses.

The photographic technique should lend itself readily to the determination of unit strains on the surfaces

of concrete beams if the accuracy of the system can be improved to the point where strains of 0.0001 inch per inch or smaller can be measured.

A more comprehensive study of the spread of plasticity should include such factors as the bond characteristics of the reinforcement and the stress-strain characteristics of the steel. A better evaluation of the strain energy due to shear would be obtained with the shearing strength of the concrete expressed as a function of the normal stress.

The determination of the deformations of reinforced concrete beams failing under any mode should be possible by strain energy methods provided all the forms of energy may be ascertained.

REFERENCES

1. American Concrete Institute Committee 318. Building code requirements for reinforced concrete. Journal of the American Concrete Institute. 27: 913-986. 1956.

2. Brock, G. Discussion of "Shear strength of two-span continuous reinforced concrete beams" by Rodriguez, Bianchini, Viest, and Kessler. Journal of the American Concrete Institute. 31: 1571-1575. 1959.

3. Baker, A. L. L. A plastic theory of design for ordinary reinforced and prestressed concrete, including moment redistribution in concrete members. London. Magazine of Concrete Research. 1: 57-66. 1949.

4. Chan, W. W. L. The ultimate strength and deformation of plastic hinges in reinforced concrete frameworks. London. Magazine of Concrete Research. 7: 121-132. 1955.

5. Ernst, George C. Plastic hinging at the intersection of beams and columns. Journal of the American Concrete Institute. 28: 1119-1144. 1957.

6. Tobiason, A. R. Photographic studies of reinforced concrete beams. Unpublished M.S. Thesis. Ames, Iowa, Library, Iowa State University of Science and Technology. 1962.

7. Smith, G. M. and L. E. Young. Ultimate flexural analysis based on stress-strain curves of cylinders. Journal of the American Concrete Institute. 28: 597-609. 1956.

8. Ramaley, David and Douglas McHenry. Stress-strain curves for concrete strained beyond ultimate load. U. S. Bureau of Reclamation, Research and Geology Division, Structural Research Laboratory Report No. SP-12. 1947.

9. Whitney, C. S. Discussion of "The plasticity ratio of concrete and its effect on the ultimate strength of beams" by Jensen. Journal of the American Concrete Institute. 39: 584-1 to 584-6. Nov. supplement. 1943.

10. Hognestad, E., N. W. Hanson, and D. McHenry. Concrete stress distribution in ultimate strength design. Journal of the American Concrete Institute. 52: 455-480. 1955.

11. Zia, Paul. Torsional strength of prestressed concrete members. Journal of the American Concrete Institute. 32: 1337-1359. 1961.

12. Balmer, G. G. Shearing strength of concrete under high triaxial stress--computation of Mohr's envelope as a curve. U. S. Bureau of Reclamation. Research and Geology Division, Structural Research Laboratory Report No. SP-23. 1949.

13. Timoshenko, S. and J. N. Goodier. Theory of elasticity. 2nd ed. New York, N. Y. McGraw-Hill Book Co., Inc. 1951.

14. Hognestad, Eivind. A study of combined bending and axial load in reinforced concrete members. University of Illinois Engineering Experiment Station. Bulletin No. 399. 1951.

15. Clark, A. P. Cracking in reinforced concrete flexural members. Journal of the American Concrete Institute. 27: 851-862. 1956.

ACKNOWLEDGEMENTS

Appreciation is expressed to Dr. Carl E. Ekberg, Jr., Professor of Civil Engineering, for assistance and guidance in carrying out this investigation.

Major credit for the completion of the testing of the beams is due to C. D. Johnson and M. C. Hsieh, Graduate Assistants. The assistance of A. R. Tobiason and J. E. Baldwin, Graduate Students, in the construction of forms and the fabrication of specimens is also recognized.

Dr. C. L. Hulsbos, formerly Professor of Civil Engineering at Iowa State University, is responsible for the initial inspiration which started this endeavor.

The many helpful suggestions offered by his colleagues are appreciated by the writer.

This investigation was made possible by a research grant from the National Science Foundation.